Boran ULUCA

THEORETICAL MODELING OF DERIVATIVES OF RGD

FATİH UNIVERSITY

The Graduate School of Sciences and Engineering

Master of Science in
Chemistry

THEORETICAL MODELING OF DERIVATIVES OF RGD

by

Boran ULUCA

July 2013

THEORETICAL MODELING OF DERIVATIVES OF RGD

by

Boran ULUCA

A thesis submitted to

the Graduate School of Sciences and Engineering

of

Fatih University

in partial fulfillment of the requirements for the degree of

Master of Science

in

Chemistry

July 2013
Istanbul, Turkey

APPROVAL PAGE

This is to certify that I have read this thesis written by Boran ULUCA and that in my opinion it is fully adequate, in scope and quality, as a thesis for the degree of Master of Science in Chemistry.

_____
Assist. Prof .Dr. Sedat COŞGUN
Thesis Supervisor

_____
Assoc. Prof. Dr. Levent SARI
Co-Supervisor

I certify that this thesis satisfies all the requirements as a thesis for the degree of Master of Science in Chemistry.

_____
Assoc. Prof. Dr. Abdülhadi BAYKAL
Head of Department

Examining Committee Members

Assist. Prof. Dr. Sedat COŞGUN _____

Assoc. Prof. Dr. Levent SARI _____

Assoc. Prof. Dr. Ali Ekrem MÜFTÜOĞLU _____

Assoc. Prof. Dr. Burak ESAT _____

Assist. Prof. Dr. Mustafa DEMİRPLAK _____

It is approved that this thesis has been written in compliance with the formatting rules laid down by the Graduate School of Sciences and Engineering.

_____
Assoc. Prof. Dr. Nurullah ARSLAN
Director

July 2013

THEORETICAL MODELING OF DERIVATIVES OF RGD

Boran ULUCA

M.S. Thesis – Chemistry
July 2013

Thesis Supervisor: Assist Prof. Dr. Sedat COŞGUN

Co-Supervisor: Assoc. Prof. Dr. Levent SARI

ABSTRACT

In this master thesis, theoretical modeling of amide and ester derivatives of arginine-glycine-aspartic acid (RGD) sequence has been studied. RGD is a small tripeptide sequence which has important role at drug delivery systems. This sequence specifically binds to α5β1 integrin proteins. In recent years, many RGD based drug delivery systems have been investigated for the development of the anti-cancer drug molecules that target these transmembrane proteins.

The Packing Parameter (P) values of the surfactant control the resulting multimolecular aggregates, and therefore it will be useful to calculate the packing parameter theoretically before the synthesis of molecules. In this study packing parameters calculated by DFT and HF methods were compared in terms of the length of the hydrophobic chains and also the bond type between hydrophobic tail and hydrophilic head group.

Keywords: Integrin, Amhiphilic Molecule, RGD, Drug Delivery Systems, Geometry Optimization, Packing Parameter, Quantum Chemical Methods.

RGD TÜREVLERİNİN TEORİK OLARAK MODELLENMESİ

Boran ULUCA

Yüksek Lisans Tezi –Kimya
Temmuz 2013

Tez Danışmanı: Yrd. Doç. Dr. Sedat COŞGUN

Eş Danışman: Doç. Dr. Levent SARI

ÖZ

Bu yüksek lisans tez çalışmasında, arjinin-glisin-aspartik asit (RGD) sekansının ester ve amit türevlerinin teorik olarak modellenmesi çalışıldı. İlaç taşıma sisteminde önemli role sahip olan RGD küçük bir tripeptit sekansıdır. Bu sekans α5β1 integrin protein ile spesifik olarak bağlanır. Son yıllarda, bu transmembran proteinini hedefleyen anti-kanser ilaç molekülü geliştirmek için birçok RGD temelli ilaç taşıma sistemi araştırılmaktadır.

Sürfaktan molekülünün kümelenme parametresi (P) değeri, sonuç multimoleküler kümelenmeyi kontrol ettiğinden dolayı kümelenme parametresinin teorik olarak molekülü sentezlemeden önce çalışılması yararlı olur. Bu çalışmada DFT ve HF metoduyla hesaplanmış kümelenme parametresi hidrofobik zincir uzunluğuna bağlı olarak karşılaştırıldı, ilaveten P değeri hidrofobik kuyruk ve hidrofilik baş grup arasındaki bağ türüne bağlı olarak hesaplandı.

Anahtar Kelimeler: Integrin, Amfifilik molekül, RGD, İlaç Taşıma Sistemleri, Geometrik Optimizasyon, Kümelenme Parametresi, Kuantum Kimyasal Metodlar,

.

To my family

ACKNOWLEDGEMENT

At the end of my thesis I would like to thank all those people who made this thesis possible and an unforgettable experience for me.

Firstly, I would like express my most sincere gratitude to my thesis supervisor to Assist. Prof. Dr. Sedat COŞGUN and Assoc. Prof. Dr. Levent SARI for their guidance and patience.

Besides my advisors, I am also grateful Tayyibe BARDAKÇI and Ayşe MARAŞLI to share her experiences and knowledge with me.

In addition, I would like to thank my dear friend Tuğba Hazal ALTUNOK and Zeynep EKİNCİ for giving a different perspective to my thesis studies and giving her interest to my study.

My greatest appreciation and friendship goes to my closest friend, Sevda AKAY who was always a great support in my life.

I would like to thank my family, especially my mother for always believing in me, for their continuous love and their supports in my decisions.

I would like to thank to Fatih University for my thesis financing.

TABLE OF CONTENTS

LIST OF TABLES

TABLE

LIST OF FIGURES

FIGURE

LIST OF SYMBOLS AND ABBREVIATIONS

SYMBOL/ABBREVIATION

Fn	Fibronectin
Gb/s	Gigabits per second
GPRC	G-protein coupled receptors
HLB	Hyrophile-Liphophile-Balanca
RGD	Arg-Gly-Asp
P	Packing Parameter
PES	Potential surface surfaces
S.E	Schrödinger Equation
VDW	Van der Waals

CHAPTER 1

INTRODUCTION

1.1 INTEGRINS

The name of integrin was given by Tamkun and Hynes in 1986 to define the receptor's function of integrating the extracellular matrix (ECM) with the cytoskeleton. They are responsible for the attachment of the cellular membrane to the ECMor other substrate.The main function of integrins includesto take part in cell signaling, and in cell motility bothdirectly and indirectly. Morever, integrins play important role in differentiation of cells, ligand recognition, tumor cell growth,apoptosis, and cancer[1].

1.1.1 Integrin Family

Integrins are member of heterodimeric transmembranecell adhesion receptors family which have non-covalent αand β subunit. Integrins havelarge extracellular and short cytoplasmic domains of 700-1100 and 30-50 residues respectively. In mammals, 18 αand 8β subunits have been encodedwhich can combine non-covalently to form 24 dimers[2].The structure of integrins was firstly investigated by electron microscopy and the headgroup of αvβ3 which was the first discovery in the integrin family. After a short period of time the crystal structure of the headgroup was discovered in association with Cilengitide[3].

The possible combinations of α and β subunits are given in the following figure.

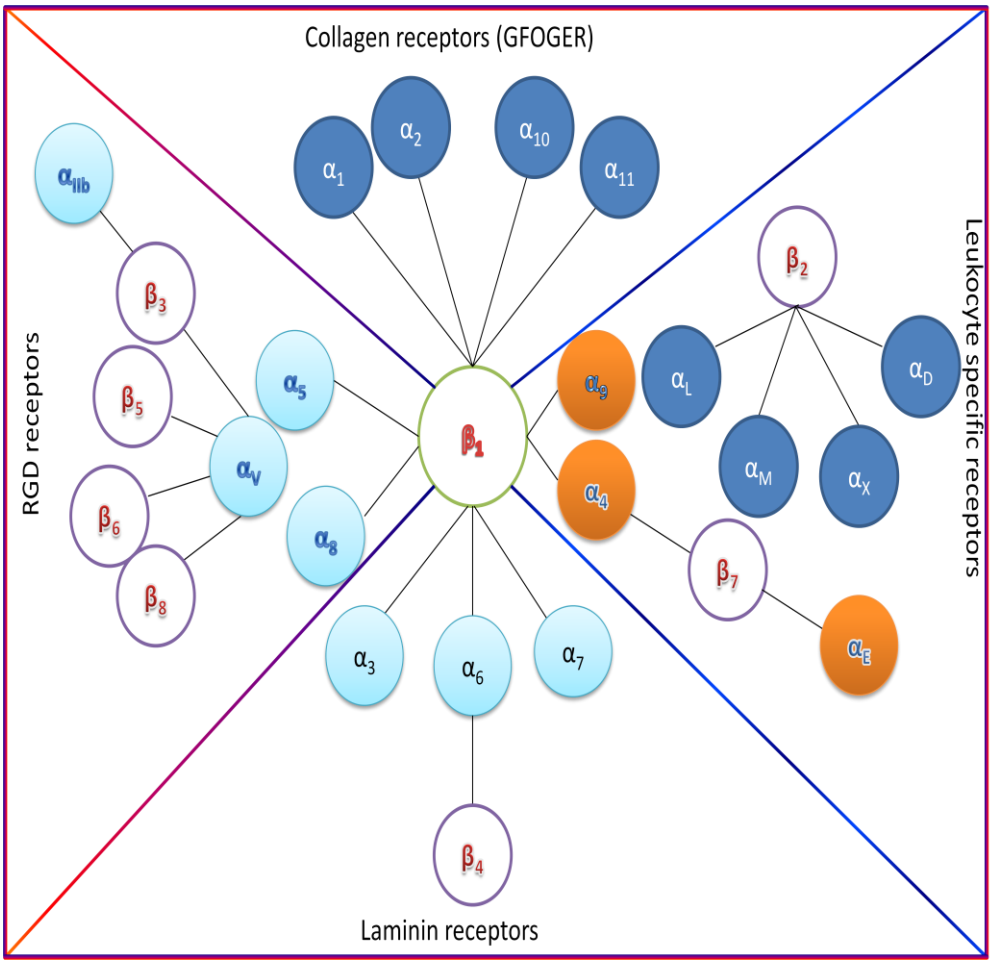

Figure 1.1 The integrin family: Combinations of α and β subunits that have been identified on cells up to now[4].

The β_1 can form dimers with at least 12 different α subunits. They are found on most vertebrate cells:$\alpha_5\beta_1$, for instance, is afibronectin receptor and $\alpha_6\beta_1$ a laminin receptor on many types of cells[5].

The $\beta_2$forms dimers with at least four types of α subunits. They are expressed only on the surface of white blood cells, where they have an essential role in enabling these cells to fight infection. The β_2 integrins primarily mediate cell-cell interactions such as the interactions between endothelial cells. People who are unable to synthesize $\beta_2$subunits have agenetic disease called Leucocyte Adhesion Deficiency . Their white blood cells lack all of the family of β_2 receptors, and they endure recurring bacterial infections[5].

The bond between the integrins and their ligands has low affinity and integrins are generally present at about tenfold to a hundredfold higher concentration on the cell[5].

1.1.2 The General Structure of Integrins

The integrins are big and complex transmembrane glycoproteins.

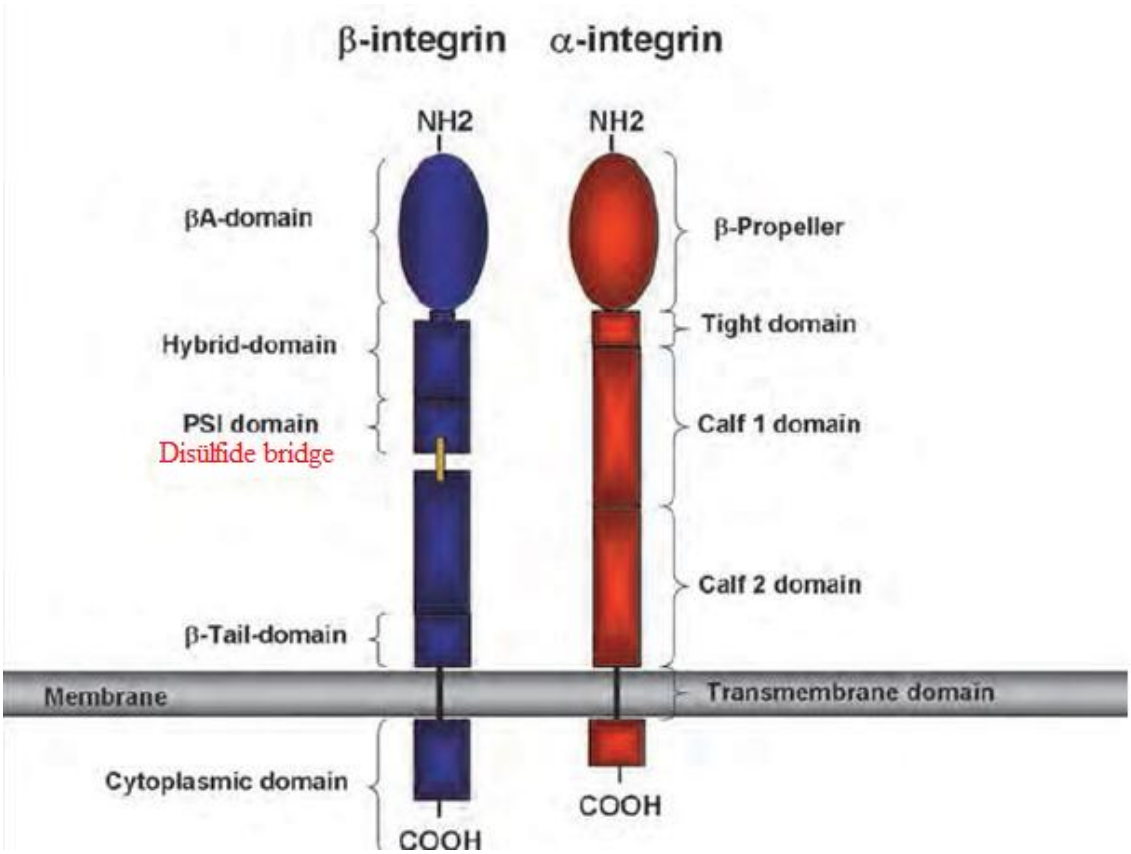

Figure 1.2 Domain architecture of the heterodimeric transmembrane domains which show howintegrins are designed to act as bidirectional signalling machines[2].

The binding of integrins to their ligands bound up withextracellular divalent cations such as Ca^{2+} or Mg^{2+}. The type of divalent cation can effect both the affinity and the specificity of the binding of an integrin to its ligands[5].

1.1.3 Integrin and Ligands

Integrins bind ligands of the extracellular matrix (ECM), such as fibronectin, collagen, laminin and vitronectin to stabilize cell attachment to the surrounding tissues or to mediate migration in the metastatic cascade.

The discovery of the RGD sequence asthe essential binding motif was the starting point for the rapiddevelopment of a variety of small-molecule a5b3-integrinantagonists with successively improving ligand characteristics and suitable in vivo characteristics for antiangiogenic therapy[6].

1.2 ARGININE-GLYCINE-ASPARTIC ACID (RGD)

The Arg-Gly-Asp (RGD) sequnce is recognized by the many integrins for example αVβ1, α8β1, αIIbβ3, αVβ3, αVβ5, αVβ6 and αVβ8[4]. This ligands can befibrinogen, fibronectin, vitronectin, collagen, and laminin. The identification of fibronectin as an ECM protein which is strongly involved in the cellular adhesion led to identification of the RGD sequence as very important recognition motif[7].

The integrins bind specifically to the RGD which have significant role in many processes for the cells.The RGDsequence was known to serve as a identification motif for integrinαVβ3over-expressed on tumor cells surface, which improved theopportunities of liposomes binding to tumor cells[8].Because αVβ3 is expressed on the tumor cells of certain types (melanoma, glioblastoma,ovarian, and breast cancer), it represents an attractive targetfor cancer therapy[6].For these reaons it is very good way to use peptidic delivery systems which include RGD sequnce for the inhibition of tumor cells.Currently, studies mainly focus on integrin αvβ3 to devise a molecular probe containing RGD for tumor imaging[9].

Figure 1.3 shows the interaction between theintegrin-covered surface and RGD vesicle.

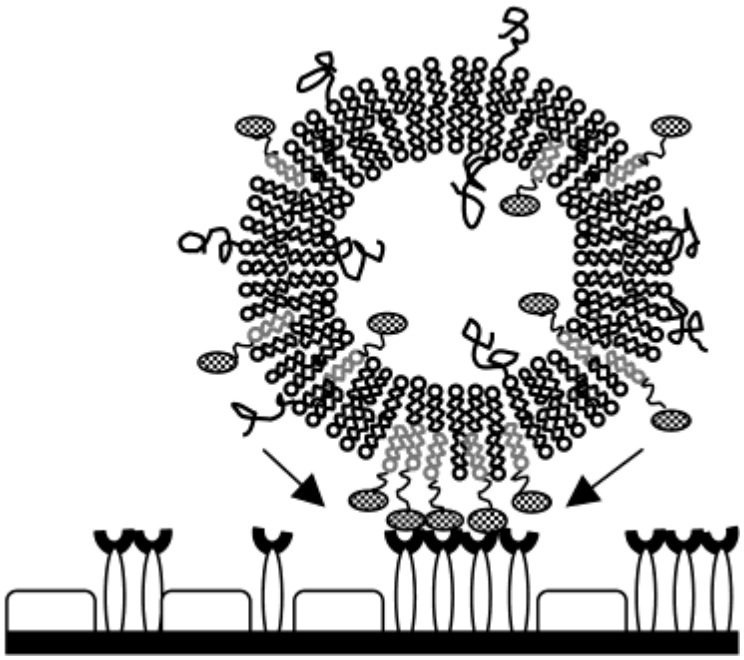

Figure 1.3 Schematic view of a RGD vesicle interacting with an integrin-covered surface [10].

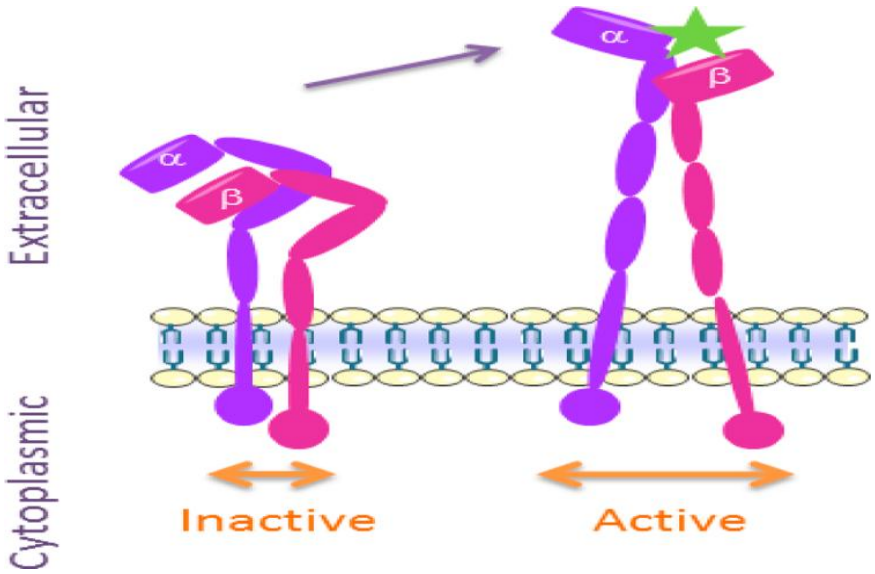

Figure 1.4 Conformational changes in αvβ3 integrin. Upon activation the extracellular domains extend and straighten, exposing the RGD binding domain [11].

The recent study about integrin activation show that the head region is pointing back towards the cell membrane and the affinity for ligands is low. The activation of integrins controll by proteins binding to the intracellular domains of the integrin and is very important for the inside-out signaling.

1.3 DRUG DELIVERY SYSTEMS

The main purpose of a drug delivery system isto design of an appropriate drug to fight the disease without any side effects.With the rise of modern science especially, organic chemistry and computational chemistry, it is possible to target specific cells or organs, therefore the harmful side effects can be reduced because of the cut down on the distribution of the drug to the non-targeted tissues[7, 12]. In addition, it is possible to protect the drugs from the unwanted reactions in the blood steram by using vesicles or globules.

The use of liposomes in drug delivery systems has a lot of advantages. Because liposomes are members of amphiphilic molecules, they can be used for the encapsulation of both hydrophobic and hydrophilic drugs with high success[12].

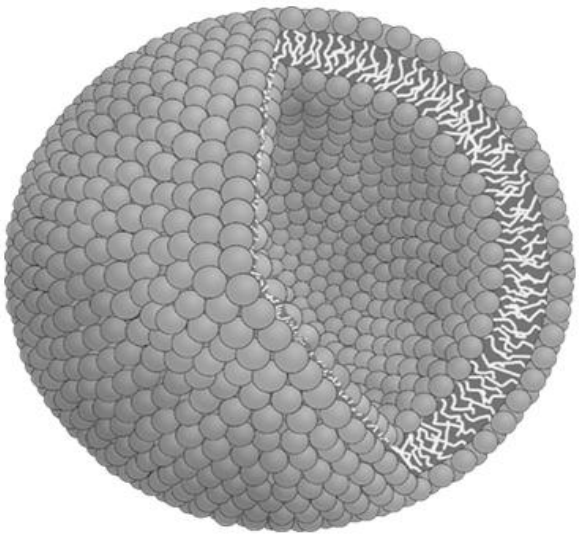

Figure 1.5A schematic representation of a liposome[12].

1.4 GEOMETRY OPTIMIZATION

Geometry optimization is a main part of many computational chemistry research projects that are related with the structure (eg. local minumum structure, global minumum structure, transition state structure etc.) and reactivity of molecules. Local minima structure is the lowest point in some limited regions of the potential energy surfaces (PES) while the global minimum is the lowest energy point anywhere on the PES [13, 14].

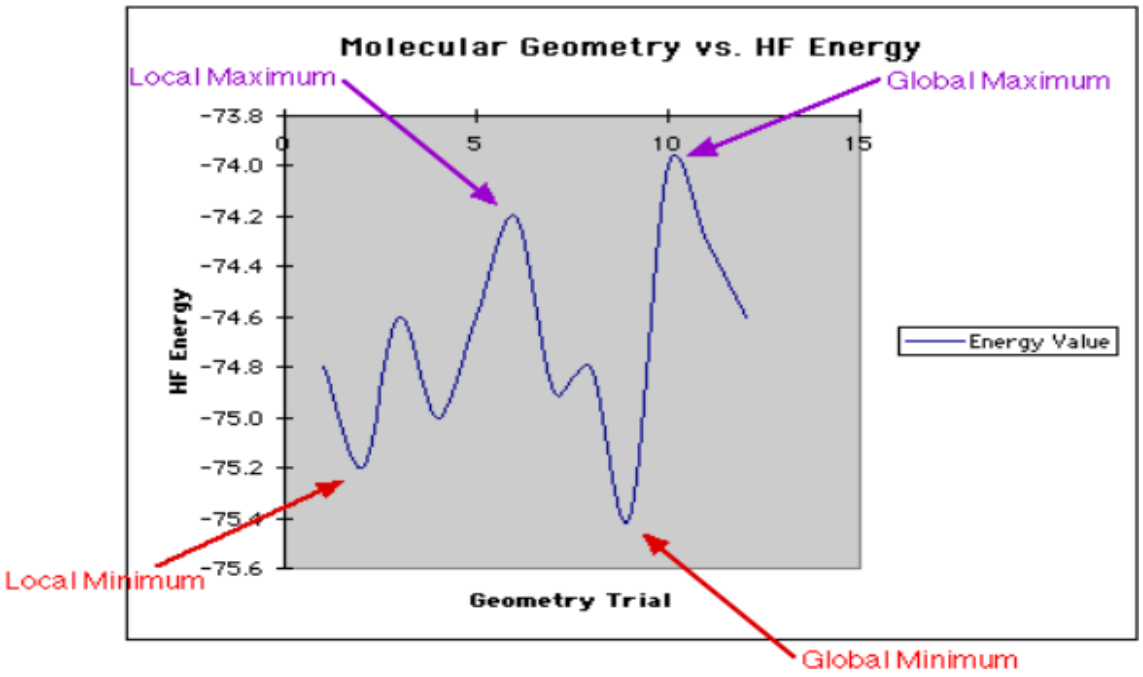

Figure 1.6A two dimensional energy graph

In order to find equilibrium structure of a system, it is necessary to calculate the minimum energy values on the PES. Geometry optimization is a technique which tests various possibilities to see which structure has the lowest energy value. Molecules are most stable when their energy is lower. (geometry optimization).

The potential energy surface can be represented by an N-dimensional plot where N is the degrees of freedom of the system [15].

For example, for a diatomic molecule H_2, the plot istwo-dimensional. The X-axis represents the internuclear separation and the energy at that bond distance on the Y-axis; in this case the PES is a curve (see Figure 1.7). At this plot there is only one parameter which is changed at the time and it has only one degree of freedom which is the bond length of H-H bond [14].

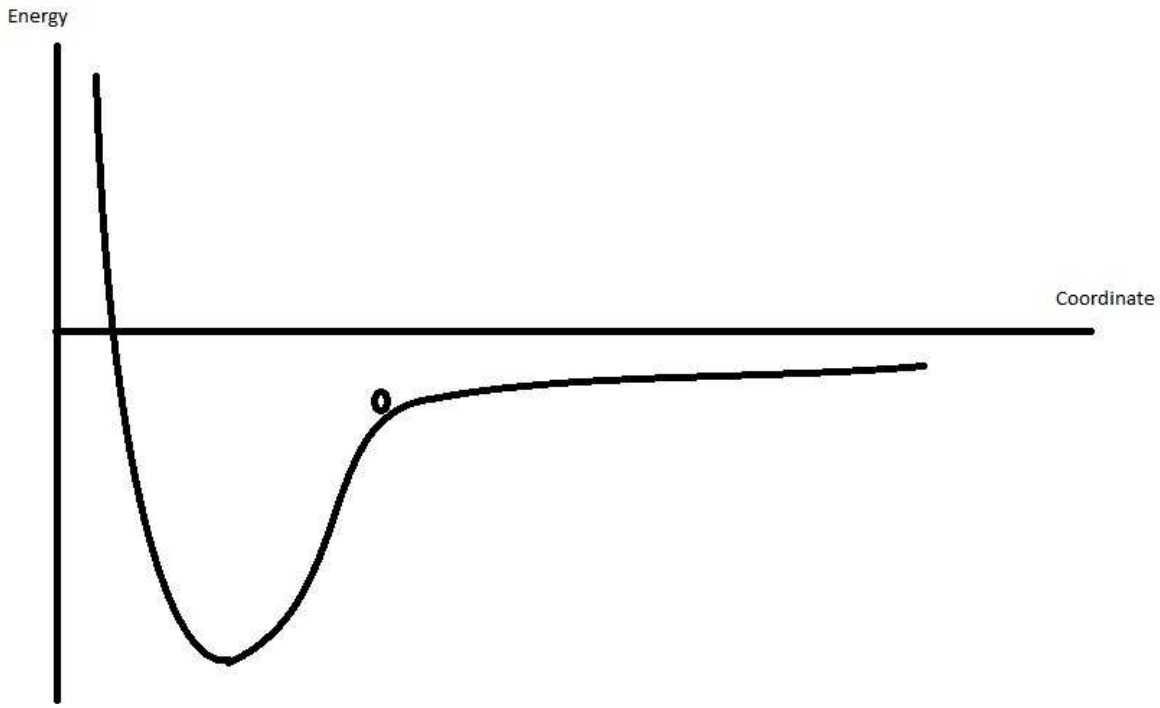

Figure 1.7 Energy surface of hydrogen molecule, H_2.

In the course of geometry optimization of H_2, thanks to the effect of the electrostatic interactions between the H atoms, the bond length of H-H bond is changed and energy is calculated. Here, H_2 tries to reach to the bottom of the well, namely the equilibrium or the lowest possible energy by making harmonic motions[15].

Most methods for effective geometry optimization depend on first derivatives of the energy with respect to coordinate and it helps to determine in which direction to move, and how far in that direction at each step of the geometry optimization. The first derivative of energy gives the gradient. At both minima and saddle points the gradient is zero. Because the negative of the gradient is vector of the forces, the forces are also zero

at such points and they are called as stationary point. The Hessian matrix or the second derivatives of the energy is also known as the force constant[14].

The main purpose of the geometry optimization is to achieve to the conformation, which is corresponding to the lowest possible energy and this process is also known as "minimization". On the other hand, geometry optimization techniques can also be used to locate local and global maxima on the energy surface. This process is called maximization and maxima are characterized by the first derivative of its energy being zero with respect to the coordinate, as it is so also for minima.

The molecular geometry has either been achieved from molecular mechanics force fields or gas phase energy minimization. It is a good approximation to the solution gas phase geometry optimization for small, relatively rigid molecules whereas to investigate the properties of a very large systems, as in biochemical applications, it is good to use molecular mechanical methods [16].

1.5 HYDROPHILE-LIPOPHILE BALANCE (HLB)

The HLB system was invented in 1949 by William C. Griffin to predict the character of surfactant molecules.

All surfactants have an oil loving portion and a water loving portion. In generally, the water loving group is a polyhydric alcohol or ethylene oxide and the oil loving group is a fatty acid or a fatty alcohol.Due to this property they have surface activity. The balance of a surfactant molecule is the ratio of the oil loving portion to the water loving portion. This balance is measured based on molecular weight[17].

$$\text{HLB}=20.\frac{Mh}{M} \tag{1.1}$$

Where*Mh* is the molecular mass of the hydrophilic portion of the molecule, and *M* is the molecular mass of the whole molecule. 0-10 HLB values correspond lipid soluble and 10-20 correspond water soluble.

1.6 PACKING PARAMETER

The self-assembly of amphiphilic molecule in a solution has been widely investigated both experimentally and theoretically. Because there are countless practical applications which are taken advantage of the resulting multimolecular aggregates[18]. The structure of these aggregates affects the properties of amphiphilic solutions. To better understand how desired structures such as micelles, flexible lamellar or vesicles can be obtained, it is important to illuminate how the how the packing shapes of packing units control the type of the resulting aggregates[18, 19].

In order to explain how the molecular organized systems form, the model of the Israelachvili can be considered. In this model, the self-assembly of amphiphiles in solution can be described by a molecular packing parameter, P given in Eq. (2), where *V* is volume of hydrophobic part, $a_0$is the surface area of head group and $l_c$is chain length of hydrophobic par [20].

$$P=\frac{V}{a_0.l_c} \tag{1.2}$$

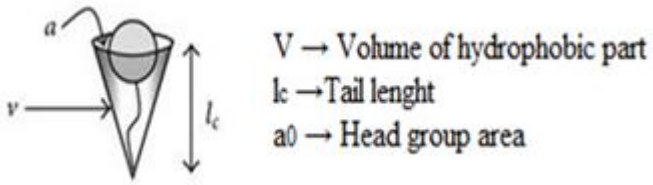

Figure 1.8 Illustration of V, l_c and a_o.

One can observe that P is directly proportional with V whereas it is inversely proportional with a_0 and l_c. To increase P, V should increase or a_0 and l_c should decrease or vice versa.

The aggregation behavior of a micelle is directly dependent on the packing parameter of the surfactant. When V/a0.lc <1/2 packing shape is often referred to as cone shape and also when V/a0.lc<1 is referred to a truncated cone whereas for

V/a0.lc≈1 the shape is referred to a cylinder and also when V/a0.lc=1 is referred to an inverted truncated cone. Israelachvili has shown that the critical packing parameter is more useful than hydrophilic-lypophilic balance number (HLB) [20, 21].

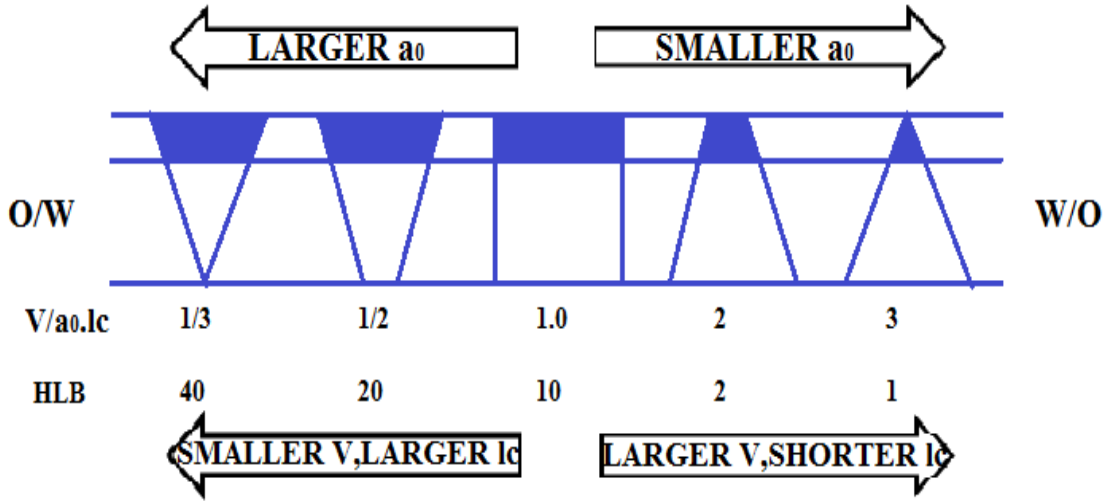

Figure 1.9 Effects of molecular moieties and solution conditionson the different types of forces acting on an amphiphilicmolecule and the resulting effect on the "packing parameter" or "shape factor", *V/a0.lc*[22].

Table 1.1 Molecular P of Israelachvili and corresponding surfactant shape.

Packing parameter	Surfactant Shape			Aggregation behavior	
P < ½	Cone			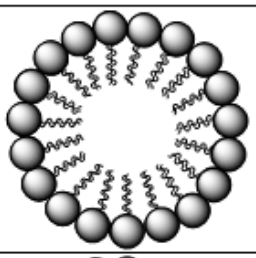	-Micelles -Hexagonal I
½ < P < 1	Truncated Cone			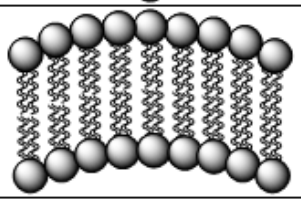	-Flexible Lamellar =vesicles
P ≈ 1	Cylinder			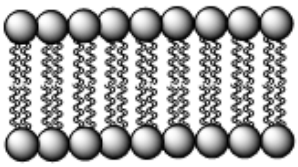	-Lamellar -Cubic
P > 1	Inverted Truncated Cone	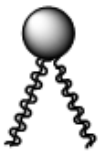		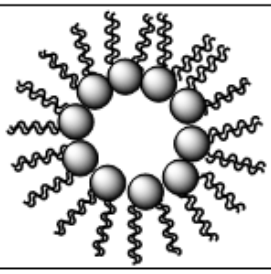	-Reversed -Micelles - Hexagonal II

The P values of the surfactant control the resulting multimolecular aggregates. For this reason it will be useful to calculate the packing parameter theoretically before synthesis of the molecule.

1.7 COMPUTATIONAL CHEMISTRY

Computational chemistry is a branch of chemistry that uses equations encapsulating the behavior of matter on an atomistic scale and use computers to solve these equations. It can be used for the identification of a new molecular entity for drug discovery, optimizing a lead compound or applications in materials research and particularly useful for systems that are hard to study by experimental techniques.

CHAPTER 2

THEORETICAL METHODS

2.1 METHODS

There is a wide variety of procedures or models have been improved to calculate molecular structure and energetics. These are usually divided into two categories, quantum mechanics models and molecular mechanics models [23]. Both approaches attempt to capture the variation of system energy associated with changes in atomic positions. Quantum mechanics provides a rigorous way to determine energy based on calculations of the electronic structure of molecules.In principle, it is accurate but usually very time-consuming even when simplifications are made (e.g., the semi-empirical methods).

In the molecular mechanics methods, which is based on the Born–Oppenheimer approximation, the calculations are not defined in detail with the electrons. It expresses the system energy just in terms of the function of the nuclear positions [24]. Molecular mechanics simulations use the laws of the classical physics wherease quantum mechanics use the laws of quantum pyhsics to analyze the properties of the molecules [25].

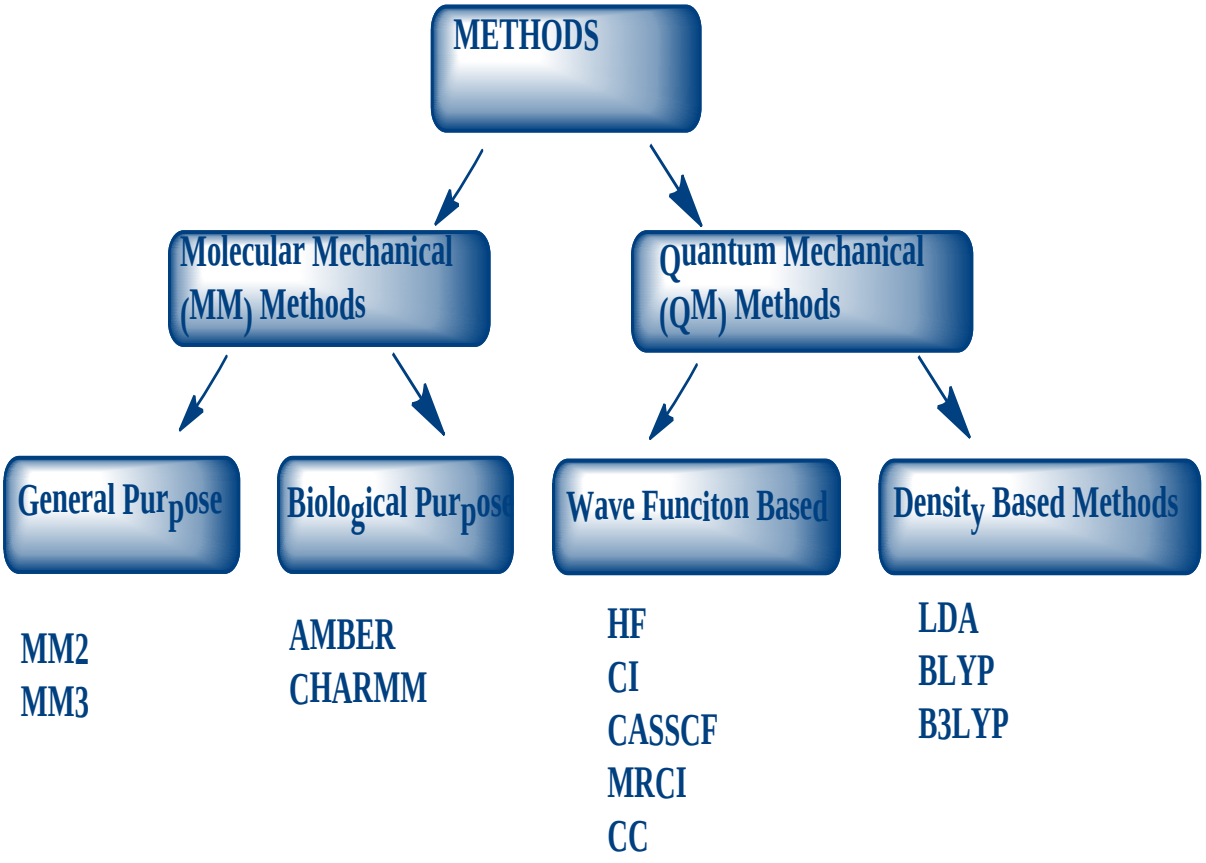

Figure 2.1 Methods for investigating molecular systems.

2.1.1 Molecular Mechanics

In order to investigate the properties of a very large system, as in biochemical applications, near molecular length scales, it is necessary to define molecules in terms of "bonded atoms" because it is not computationally practicable to use solely quantum mechanical approach to compute potential energies [23, 24, 26].

In this method, the total potential energy, E, can be expressed as a sum of Taylor series expansion;

$$E = E_{str} + E_{bend} + E_{tors} + E_{vdw} + E_{el} + E_{cross}\ [27]. \quad (2.1)$$

where E_{str}, E_{bend}, Et_{ors}, E_{vdw}, $E_{el,}$ and E_{cross}. are energies associated with stretching for every pair of bonded atoms and bending, torsional energy, Van der Waals energy, electrostatics, and cross terms respectively. The equations for each term of total potential energy include parameters which are specific for the interaction between the atoms and force field is called for these specified set of equations and parameters [26]. A schematic illustration of each energy term and the corresponding bond structure of a graphene cell is shown in Figure 2.2. In order to better understand the methodology, we shortly discuss these energy terms in the following.

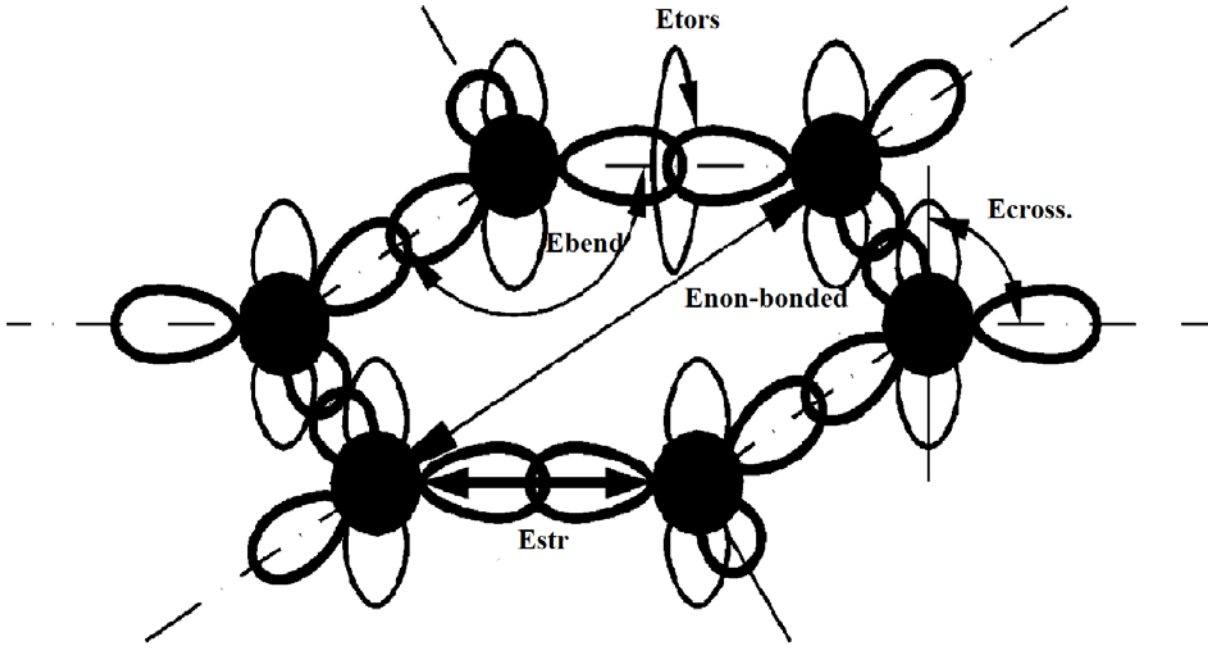

Figure 2.2. Bond structures and corresponding energy terms of a graphene cell [24].

2.1.1.1 Bond Stretching Energy and Bending Energy

The stretching energy for bonded A and B atoms represents the energy required to stretch or compress. It is most simply given in terms of quadratic (“Hook’s law”) forms. Bending energy terms are treated very similarly to stretching energy and associated with the required energy to displacement of the bond angle from the equilibrium angle, θ.

$$E_{str}(r) = 1/2\ k_{s,ij}\ (\ r_{ij} - r_o\ )^2 \qquad (2.2)$$

$$E_{bend} = 1/2\ k_{b,ijk}\ (\theta_{ijk} - \theta_o)^2 \qquad (2.3)$$

For the Eq. (2.2) where $k_{s,ij}$ is the empirical force constant for the bond, *rij* is the distance between the two atoms, and r_0 is the equilibrium bond length which is specific for each type of bonds (C-O, C-H, N-C,…). For the Eq. (2.3), $k_{b,ijk}$ is the empirical bending force constant and θ_{ijk} is the actual bond angle and θ_0 is natural bond angle.

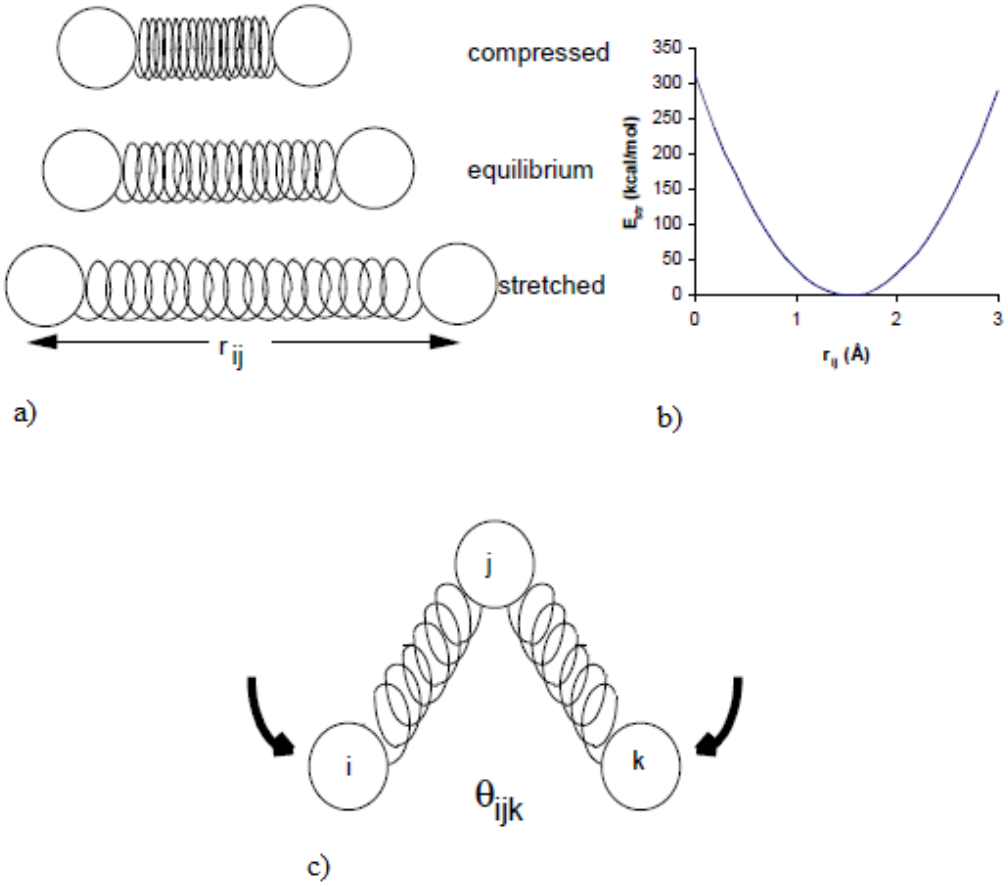

Figure 2.3 (a) The compressed, equilibrium and stretched form of a diatomic molecule and (b) their energies, (c) bond bending [28].

When a bond is bent stretch-bend interaction takes into account and because of the coupling between stretching and bending the two bond lengths increase. Figure 2.3 shows this increasing schematically.

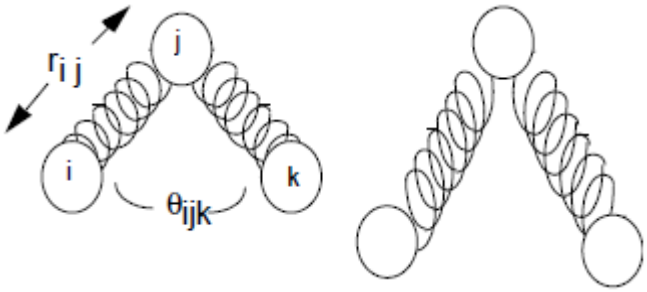

Figure 2.4. Stretch-Bend Interaction.

2.1.1.2 Torsional Energies

The torsional energy is used to correct the remaining energy terms rather than to represent a physical process. Therefore, the torsional potential is not necessary in all molecular mechanics.

2.1.1.3 Non-Bonding Energies:

The non-bonding energies imply the energy between the atoms i and j which are not linked by covalent bonded. It is divided into two groups, one of them is Van der Waals (VDW) interaction and the other is Coulombic interaction. The total non-bonding interaction can be written as the sum. of the VDW energy and Coulombic interaction, which given in following equation.

$$E^{\text{non-bonded}}(r) = E^{\text{VDW}}(r) + E^{\text{Coulombic}}(r) \quad (2.4)$$

Lennard-Jones potential which is one of the well known empirical function for the VDW force is also represented as “12-6” and it can be written as in the following formula;

$$E^{\text{VDW}}(r) = A/rij + B/rij \quad (2.5)$$

where *A* and *B* are constants which depend on identities of the two atoms and r_{ij} is the distance separating the two nuclei. The formula for the Colulombic interaction is as below;

$$E^{\text{Coulombic}} = kqq/r \quad (2.6)$$

where *k* is Coulomb's constant, *r* is the distance between atoms j and i and the point charge of atoms reperesented by qj and qi. this interaction occurs when the molecular bond is polar and atoms have the partial charge.

2.1.2 Quantum Mechanics

Quantum mechanical methods are based on the solving of the Schrodinger Equation (S.E.) for a given system to determine the energy and other related thermodynamics properties.

$$H\Psi = E\Psi \tag{2.7}$$

Where Ψ is the wave function which include all informations that can possibly be known about the quantum system at hand, *E* is electronic energy of a system and *H* is the Hamiltonian operator.

It is very difficult to solve the S.E. without any approximation for the two or more electron systems. Therefore there is a wide variety approximation for it.

2.1.2.1 Hartree-Fock Approximation

The Hartree-Fock Approximation plays a central role in chemistry since and it is the origin for most methods which describe the many-electron system more accurately [29].

The assumption behind this approximation is that electrons in an atom move independently toward the other electrons. HF approximation assumes that the wave function of a system which satisfy the anti-symmetry condition like fermions, can be written with single Slater determinant;

$$\Psi(r_1, r_2,\ldots..r_i\ldots r_j\ldots r_N) = - \Psi(r_1, r_2,\ldots..r_j\ldots r_i\ldots r_N) \tag{2.7}$$

where *r* is position of electron i.

This theory is very useful for computing the structure of a system and predicting some properties (equilibrium energy and vibrational frequency…).But it ignores electron correlation.

However good the HF ground-state wave function may appear to be, it is not the ‘exact’ wave function. The Hartree–Fock method relies on averages: it does not consider the instantaneous coulombic interactions between electrons; nor does it take into account the quantum mechanical effects on electron distributions because the effect of the n – 1 electrons on the electron of interest is treated in an average way. We summarize these deficiencies by saying that the HF method ignores electron correlation. A great deal of modern work in the field of electronic structure calculation take aim at taking electron correlation into account.

The ab initio methods described above all start with the Hartree–Fock approximation in that the HF equations are first solved to find spinorbitals that can then be used to construct configuration state functions. These methods are widely used by quantum chemists today. However, they do have limitations, in particular the computational difficulty of performing accurate calculations with large basis sets on molecules containing many atoms and many electrons.

2.1.2.2. Density Function Theory

Density Functional Theory (DFT) is an exceptional theory which allows to modify complicated N-electron wave function and its Schrödinger equation by the more basic electron density $\rho(r)$

In the Density Functional Theory (DFT) the molecular properties can be solved by using electron probability density, ρ, which is a function of space and time, instead of molecular wave function [30]. Because the density is a physical observable it is very suitable variable and it solely depends on three spatial (x,y,z) coordinates, on the other hand the many-body wave function depends on 3N spatial coordinates which are coordinates of each N atoms in the related system [25]. It is signed that the electron density of any system uniquely determines each ground-state properties of the system in this theorem [31].

The exact ground state energy electron density is given by;

$$\rho(r) = \sum_{i=1}^{n} |\psi_i(r)|^2 \tag{2.8}$$

Some properties of the electron density;

I. The meaning of ρ(r) is the number of electrons per unit volume in a given state
II. It is a physical observable and it can be measured by using X-ray dif raction,
III. It solely depends on x,y,z coordinates,
IV. Because of the it is square of Ψ, it is non-negative funciton,
V. The electron density has a finity value at any atomic nucleus in an atom, molecule or solids while the limit of ρ(r) is zero at infinty,

$\rho(r \rightarrow \infty) = 0$ [32].

The ground-state electronic energy can be written as the following formula;

$E = E_T + E_V + E_J + E_{XC}$ [23].

Where E_T is kinetic energy, E_V is electron-nuclear interaction energy, E_J is Coulomb energy, and Exc is exchange/correlation energy. Except for ET, all energy components based on the total electron density, ρ(r).

It can be used to do calculations on molecules of 100 or more atoms in significantly less time than these HF methods. Furthermore, for systems involving d-block metals, DFT yields result that very frequently agree more closely with experiment than HF calculations do [26].

This is fundamentally different from quantum chemical models, which make no reference whatsoever to chemical bonding [33].

CHAPTER 3

RESULTS AND DISCUSSION

3.1 THE STRUCTURE OF THE OPTIMIZED MOLECULES

In this thesis, two different RGD derivatives according to the bond type (between the hydrophobic tail and hydrophilic head group) are studied; amide and ester derivatives. There are some differences betweeen the amide and ester bonds and these differences effect the tail lenght and possible tail position. In this regard, the changing of the bond type changed the volume of hydrophobic part and packing parameter even if they have same number of carbon in the tail. The main aim of this thesis is calculation of P values of ester and amide derivatives of RGD and after calculation part compare the aggregation behaviour theoretically. Based on this information it is believed that the theoratical calculations of P values help to synthesize desired structure for the desired aggregation type.

In this study, 10 different derivatives of RGD are investigated. Five of them are amide derivatives and others are ester derivatives and all molecules have same hydrophobic head group. Both the ester and amide derivatives have 10, 12, 14, 16 and 18 carbons in the hydrophobic chain. All derivatives are analysed with two different quantum chemical methods; HF/6-31 and B3LYP/6-31. The following figure shows the abbrevations for all these molecules.

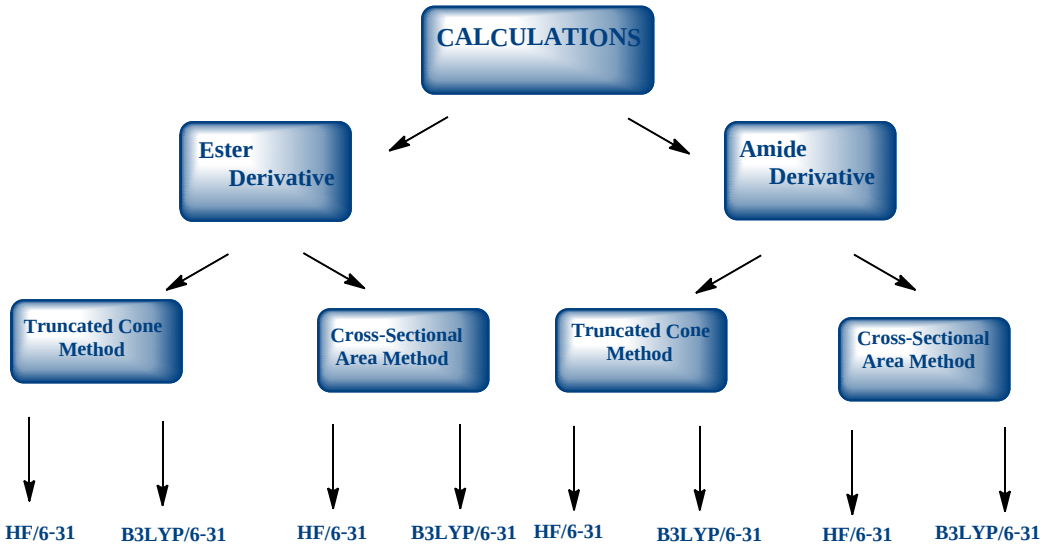

Figure 3.1 The using calculations methods.

Table 3.1 Abbrevations for all RGD derivatives.

	ESTER DERIVATIVES		AMIDE DERIVATIVES	
Number of C	**HF/6-31**	**B3LYP/6-31**	**HF/ 6-31**	**B3LYP/6-31**
10	C10-HF	C10-DFT	aC10-HF	aC10-DFT
12	C12-HF	C12-DFT	aC12-HF	aC12-DFT
14	C14-HF	C14-DFT	aC14-HF	aC14-DFT
16	C16-HF	C16-DFT	aC16-HF	aC16-DFT
18	C16-HF	C18-DFT	aC18-HF	aC18-DFT

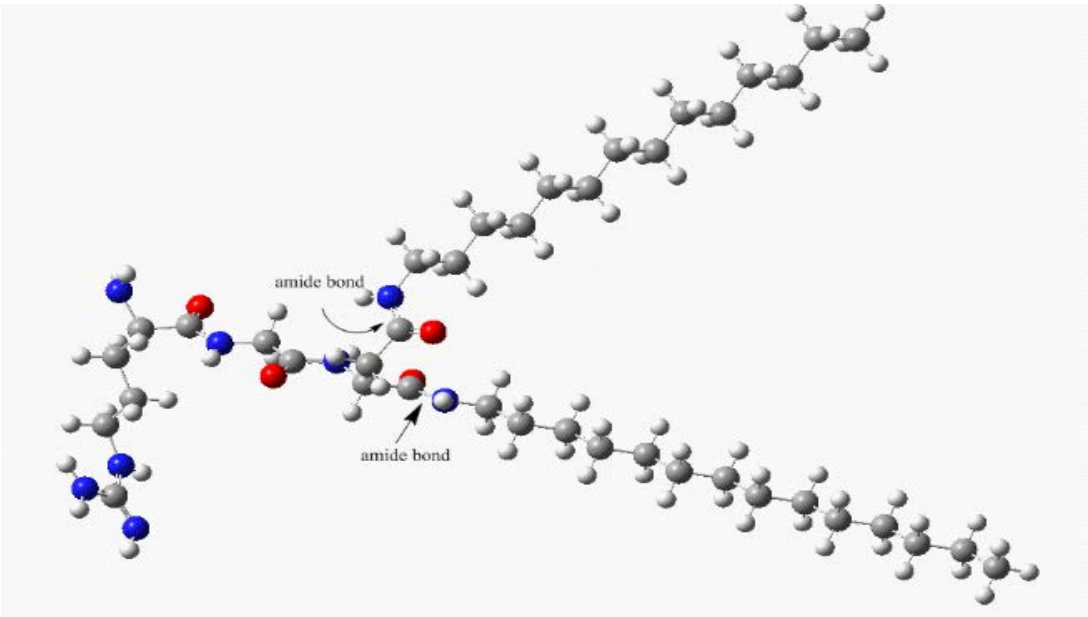

Figure 3.2 One of the amide derivatives of RGD (aC14).

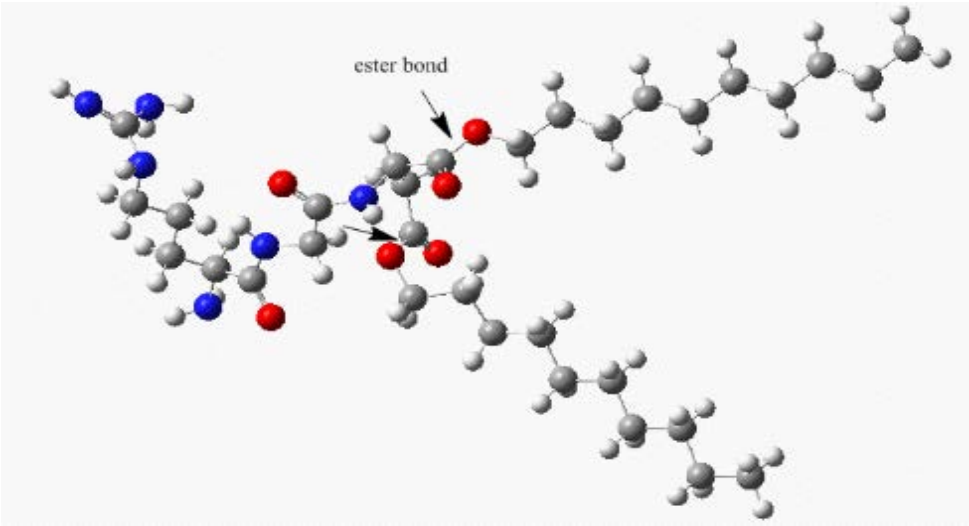

Figure 3.3 One of the ester derivatives of RGD (C10).

As shown in the Figure 3.4, the amide bond has partial double bond character i.e. 40% C-OH=N-(imine). This results in a shorter bond length, and increased bond order. Ester bonds do not have this phenomenon of electron delocalisation. Since partial double bonds are stronger than single ester bonds, overall greater stability results in proteins. And also, unlike amide bonds, ester bonds provide the flexiblity of the

molecules. Because the C-O-C bonds has a lower rotational barrier, the flexibility defines their pysical properties. In our study, we would like to compare the molecules which include amide and ester bonds for drug delivery systems. To this end, it is important to support experimental data with theoretical data for illustrating the surface morphology.

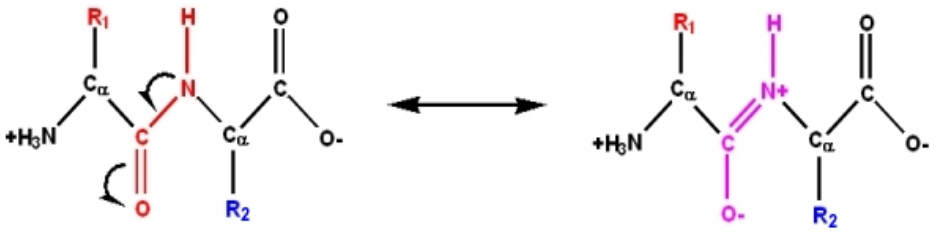

Figure 3.4 Partial double bond character of amide bond [1].

All caculations in this thesis were performed by Gaussian03 and the visualization parts were done with GaussView 3.0 program. The optimized molecular structure of the ester derivatives of RGD were investigated using quantum mechanical methods which are DFT with B3LYP method and 6-31G basis set and HF method with same basis set; (HF/6-31and B3LYP/6-31

The calculations consist of two steps. At the first step initial structure of molecule is given as a input file for the geometry optimization with HF/6-31 basis set. The resulting molecular structure of this optimization is used for the second step as input file with B3LYP/6-31 basis set.

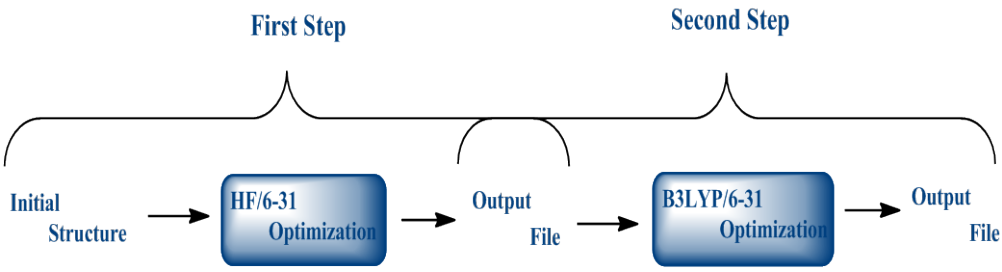

Figure 3.5 Calculation steps.

The following figures are gas-phase optimized structure at HF and DFT respectively.

Note: Color code of the atom types placed in the snapshots of the simulation systems are as follow. Carbon: Gray, Nitrogen: Blue, Oxygen: Red, Hydrogen: White.

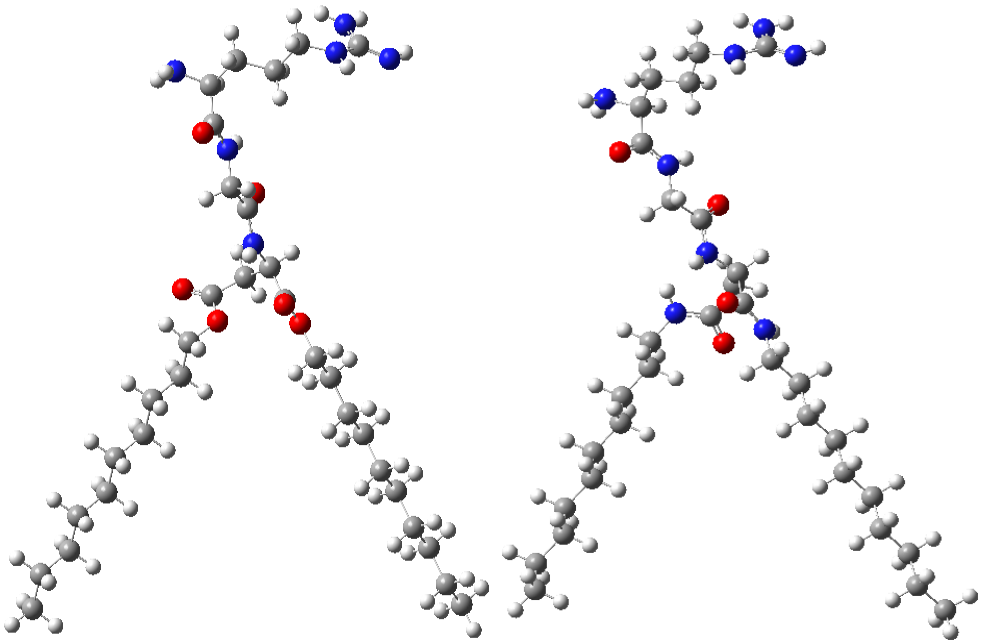

(a) (b)

Figure 3.6 C10-HF (a) ester (b) amide.

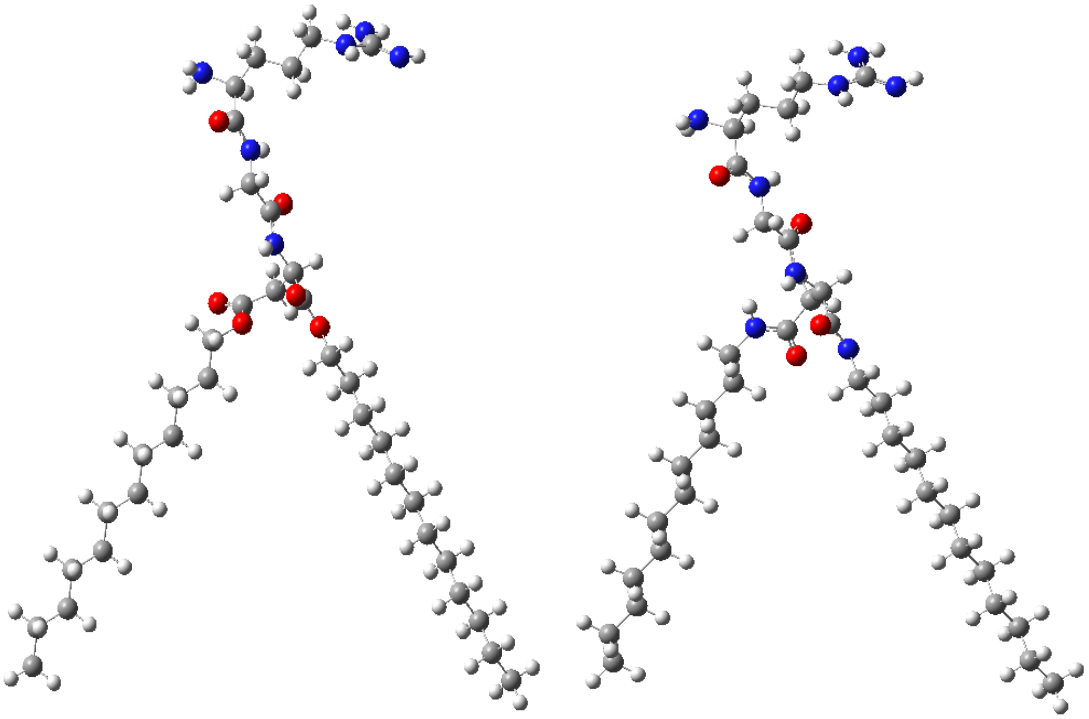

(a) (b)

Figure 3.7 C12-HF (a) ester (b) amide.

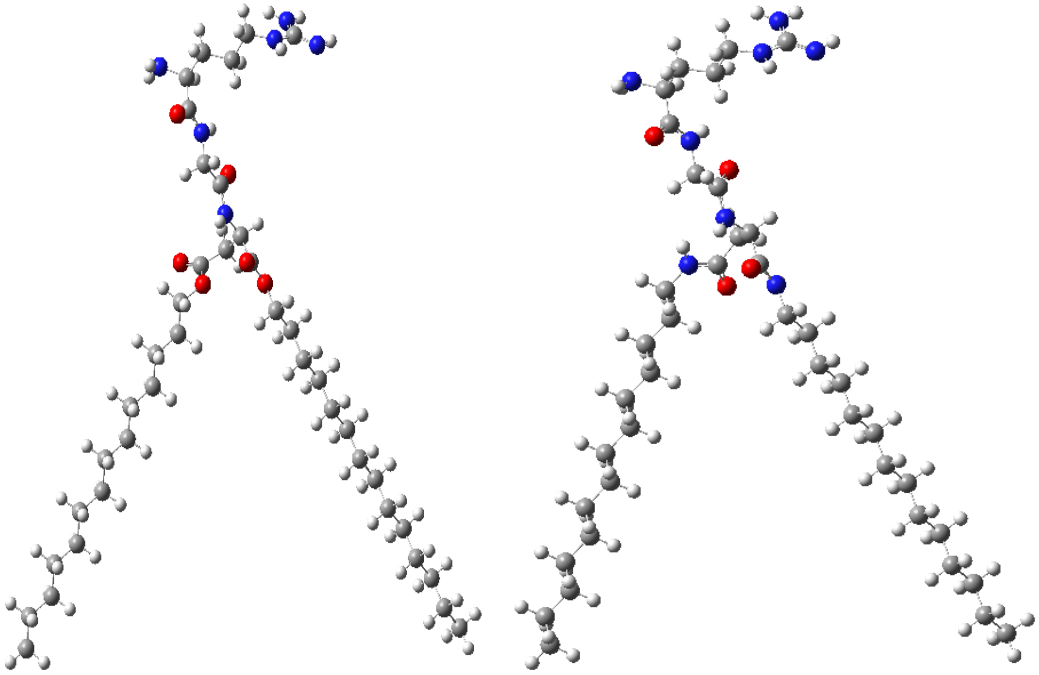

(a) (b)

Figure 3.8 C14-HF (a) ester (b) amide.

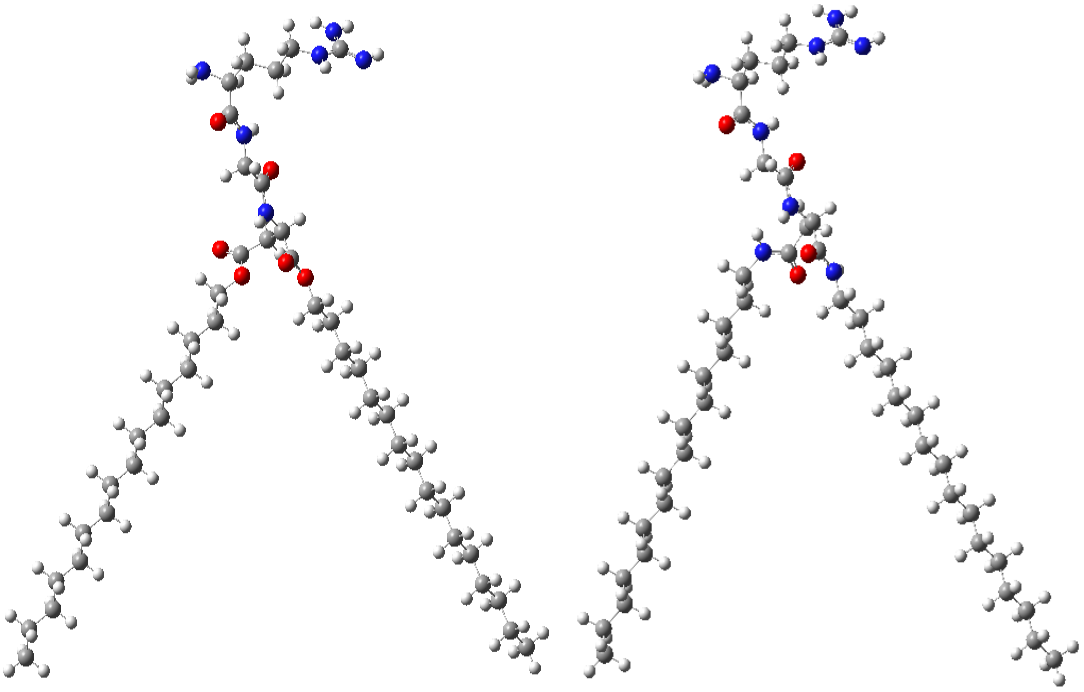

(a) (b)

Figure 3.9 C16-HF (a) ester (b) amide.

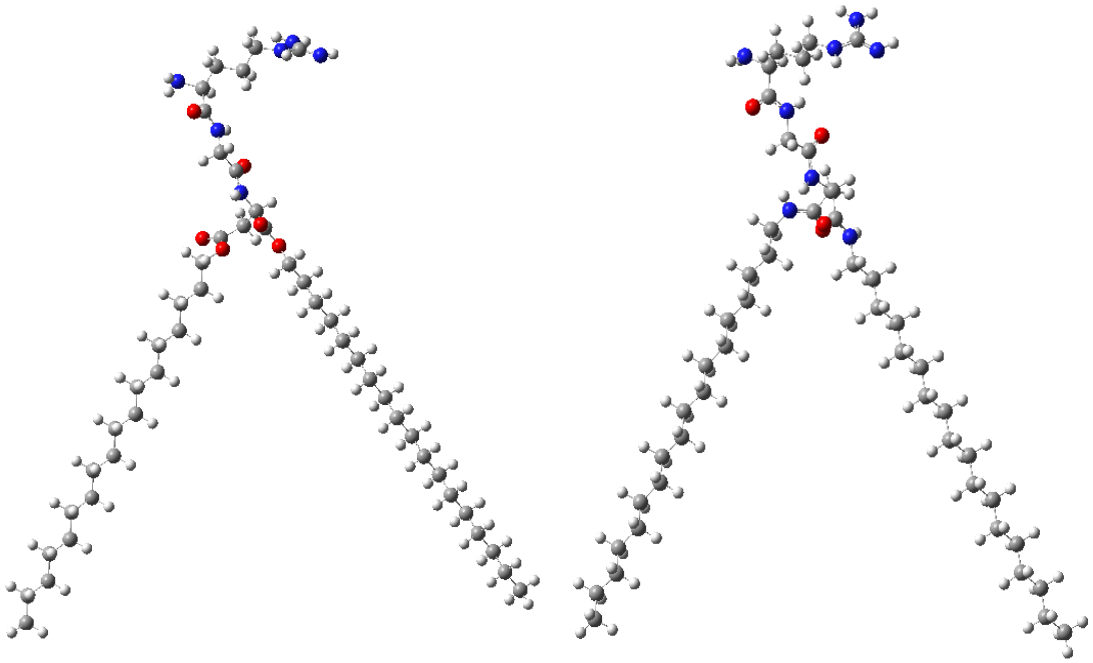

(a) (b)

Figure 3.10 C18-HF a) ester (b) amide.

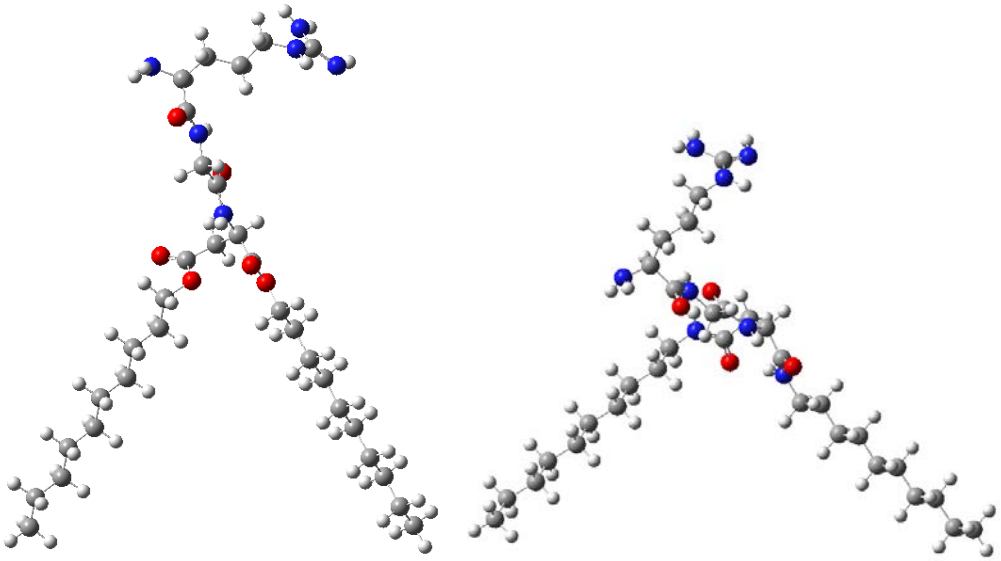

(a) (b)

Figure 3.11 aC10-DFT (a) ester (b) amide.

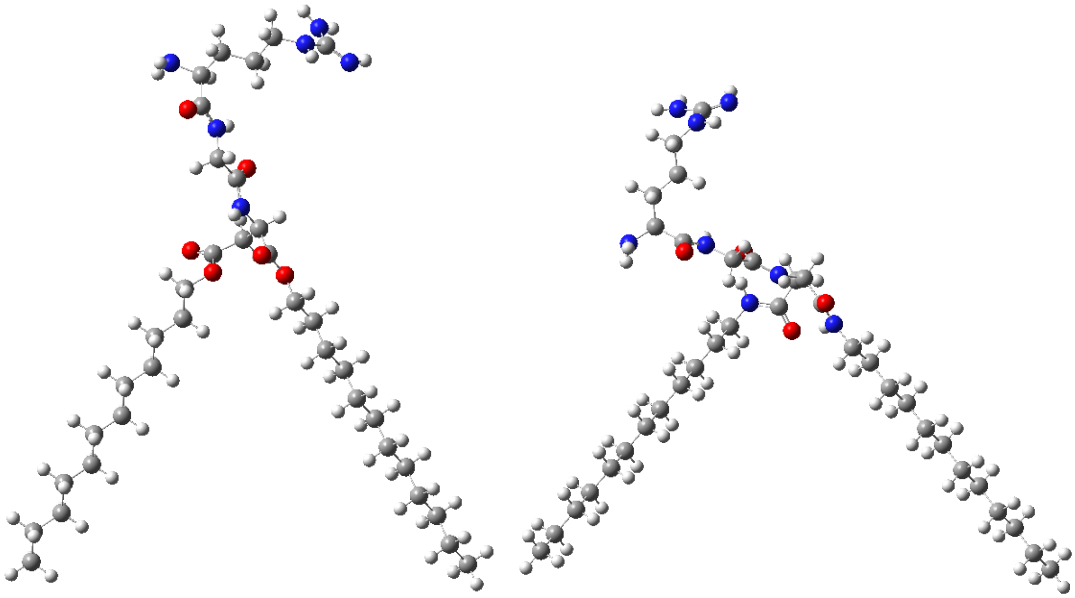

(a) (b)

Figure 3.12 aC12-DFT (a) ester (b) amide.

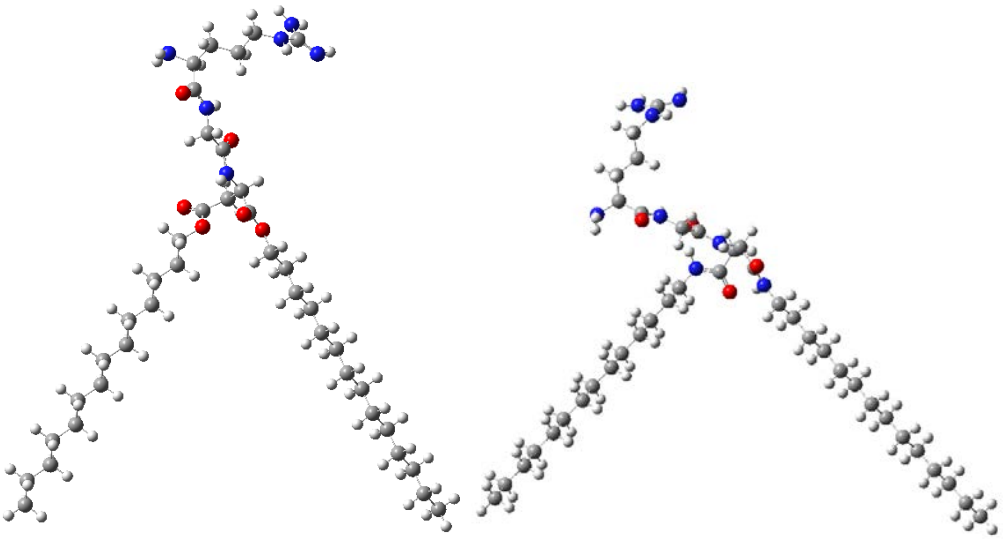

(a) (b)

Figure 3.13 aC14-DFT a) ester (b) amide.

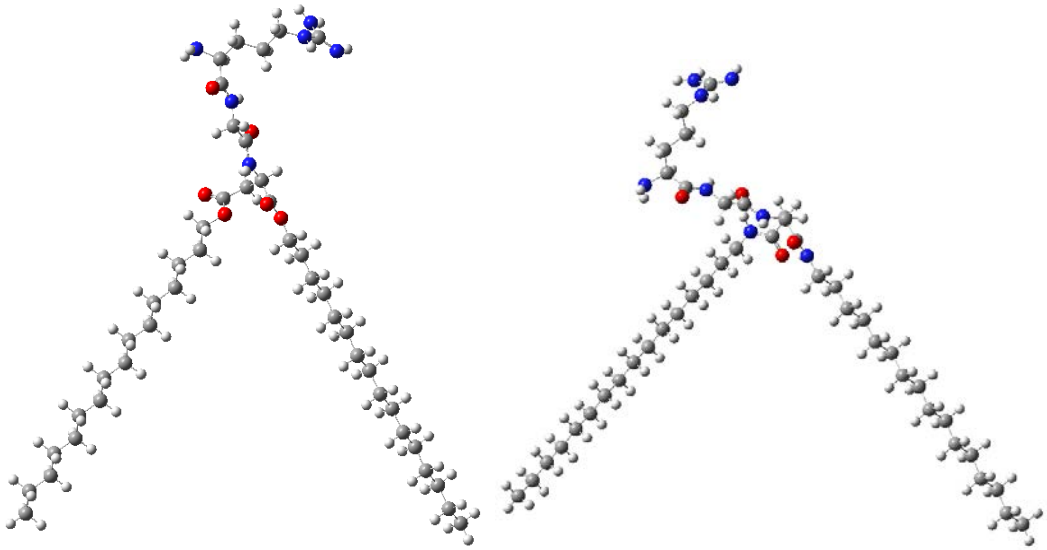

(a) (b)

Figure 3.14 aC16-DFT a) ester (b) amide.

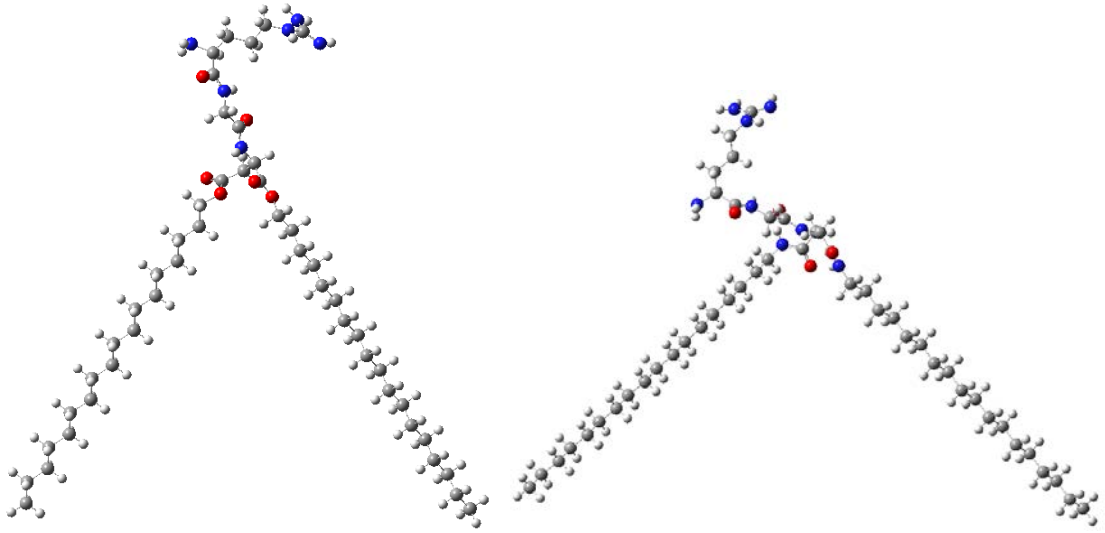

(a) (b)

Figure 3.15 aC18-DFT a) ester (b) amide.

After optimization, the tail length of both ester and amide derivatives are measured. Considerable differences are not observed between them. For example, 10-C derivatives have 14.89 **(**Å) tail length both ester and amide derivatives. The biggest difference is observed (0.12) in the 14-C. But in the following section will be seen that whether the V, l_c, a_0 and P values are different or not.

Table 3.2 The tail lenght (Å) of the all RGD derivatives.

Tail Length (Å)	**Ester/HF**	**Amide/HF**	**Ester/DFT**	**Amide/DFT**
10-C	14.89	14.89	14.98	14.96
12-C	17.44	17.42	17.55	17.55
14-C	20.00	19.97	20.13	20.01
16-C	22.56	22.52	22.7	22.73
18-C	25.1	25.08	25.26	25.27

3.2 CALCULATED V, a_0, l_C AND P VALUES OF DERIVATIVES OF RGD

After optimization, the volume of hydrophobic part has been calculated with two different methods. First one is truncated cone and the other is cross-sectional area method. In the first method the tails are fitted into a truncated cone and hyrophobic volume is calculated for one surfactant molecule, in the second method the tails are fitted into a trapezium and the maximum surfactant per unit volume is calculated. And also, the water effect is considered in the second method.

3.2.1. Truncated Cone Methods

Packing parameters are calculated by using optimized geometric structure. In order to calculate P values for the derivatives of RGD, the tail was fitted into a truncated cone (Figure 3.16) and the head group into a rectangle. The van der Waals radii for each atom were taken into account in the calculation.

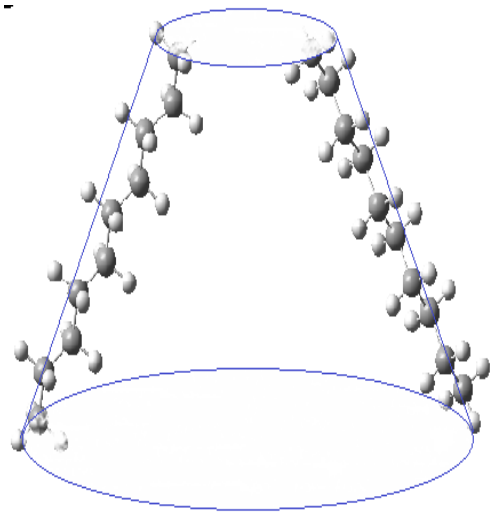

Figure 3.16 Fitting of hyrophobic tail in the truncated cone.

$$P = \frac{V}{a_0 . l_c} \tag{3.1}$$

All calculations are made as follows; the tail height, head group area and volume of C10-HF were 13.65 Å, 168.79 $Å^2$ and 2497.03 $Å^3$ respectively, and thus the

calculated value of the geometrical packing parameter was P= 2497.03/13.65×168.79=1.08

The P values of ester derivatives change between the 1.08-2.15 and 1.12-2.18 with HF and DFT respectively. And also, for amide they change between the 1.05-1.98 and 1.73-3.22 with the HF and DFT respectively in the Truncated Cone Methods.

Becher has shown that HLB number and P values are consistent with each other, they should be examined together for this reason HLB values are written into the tables.

Table 3.3 The calculated V, a_0, l_c and P values of ester derivatives of RGD with HF.

Number of C	**V ($Å^3$)**	**a_0 ($Å^2$)**	**l_c (Å)**	**P**	**HLB**
C10	2497.03	168.79	13.65	1.08	11.06
C12	3496.42	166.54	15.83	1.32	10.15
C14	4660.42	164.95	18.16	1.55	9.37
C16	5885.83	164.95	20.83	1.71	8.71
C18	8016.83	166.54	22.35	2.15	8.13

Table 3.4 The calculated V, a_0, l_c and P values of amide derivatives of RGD with HF.

Number of C	**V ($Å^3$)**	**a_0 ($Å^2$)**	**l_c (Å)**	**P**	**HLB**
aC10	2432.93	165.04	14.06	1.05	11.00
aC12	3054.58	165.15	16.51	1.12	10.03
aC14	4503.75	164.95	18.54	1.47	9.31
aC16	5697.61	166.54	20.92	1.63	8.65
aC18	7527.72	164.83	23.03	1.98	8.07

As shown in the above tables, P, V and l_C values linearly increase with the increasing of the tail length and the head groups area are independent of tail lenght, they are nearly the same for all derivatives. In contrast to DFT results, in the truncated cone methods at HF the P values of ester derivatives are relatively bigger than the amide derivatives. But, as in shown in the following tables, the amide derivatives have bigger P values at DFT.

Table 3.5 The calculated V, a_0, l_c and P values of ester derivatives of RGD with DFT.

Number of C	**V (Å^3)**	**a_0 (Å^2)**	**l_c (Å)**	**P**	**HLB**
C10	2547.65	165.04	13.76	1.12	11.06
C12	3558.57	165.15	15.98	1.34	10.15
C14	4813.65	164.95	18.19	1.60	9.37
C16	6282.57	166.54	20.35	1.85	8.71
C18	8136.88	164.83	22.57	2.18	8.13

Table 3.6 The calculated V, a_0, l_c and P values of amide derivatives of RGD with DFT.

Number of C	**V (Å^3)**	**a_0 (Å^2)**	**l_c (Å)**	**P**	**HLB**
aC10	3706.96	172.70	12.39	1.73	11.00
aC12	4765.24	175.21	15.29	1.77	10.03
aC14	6467.22	176.35	17.07	2.15	9.31
aC16	8031.86	175.18	19.86	2.31	8.65
aC18	11440.27	176.35	20.14	3.22	8.07

The flexibility of the ester bond provides attraction between two hydrocarbon chains of amphiphilic molecule, while amide bond prevents it because of rigidity of amide bond. Additionally, due to free rotation of the ester bond in the liquid the volume of them get smaller.

Hydrophilic-lipophilic balance (HLB) value which is the oldest method for describe the aggregation behaviour of amphiphilic molecules, is very useful because it allows a prediction of the aggregation behaviour. But this method does not consider the bond type, it considers the molecular mass of different part.The method of Israelachvili which is based on molecular packing parameter, P allows us to compare the bond types effect under the different bond conditions. Our studies have shown that while the HLB values of ester and amide derivatives are nearly the same their molecular packing parameters are very different. And also molecular geometries are very different. Based on this different packing parameters it can be said that they should have different aggregation type. Figure 3.15 support this result because their molecular geometries are very different.

3.2.2 Cross-Sectional Area Methods

In the cross-sectional area methods, the ester derivatives of RGD calculated with two different quantum chemical methods. First table is HF result with 6-31G basis set. And the other table is DFT result with B3LYP method and same basis set. In order to calculate P values for the derivatives of RGD, the tail was fitted into a trapezium and given depth and the head group fitted into a rectangle. The van der Waals radii for each atom were taken into account in the calculation.

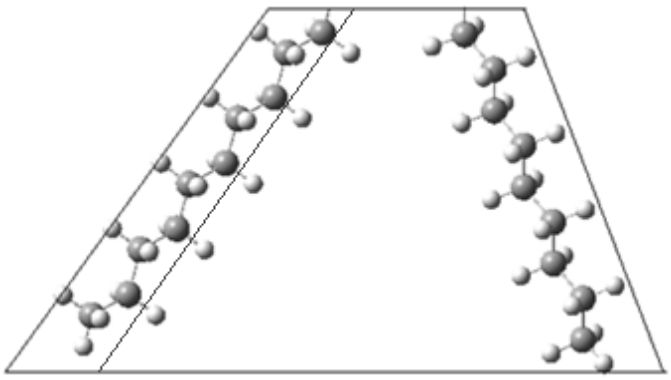

Figure 3.17 Fitting of hyrophobic tail in the trapezium.

Table 3.7 The calculated V, a_0, l_c and P values of ester derivatives of RGD with HF.

Number of C	**V (Å^3)**	**a_0 (Å^2)**	**l_c (Å)**	**P**	**HLB**
C10	1106.21	168.79	13.65	0.48	11.06
C12	1400.22	166.54	15.83	0.53	10.15
C14	1724.09	164.95	18.16	0.57	9.37
C16	2077.48	164.95	20.83	0.60	8.71
C18	2518.34	166.54	22.35	0.67	8.13

Table 3.8 The calculated V, a_0, l_c and P values of amide derivatives of RGD with HF.

Number of C	**V (Å^3)**	**a_0 (Å^2)**	**l_c (Å)**	**P**	**HLB**
aC10	1116.45	165.04	14.06	0.48	11.00
aC12	1350.59	165.15	16.51	0.49	10.03
aC14	1723.79	164.95	18.54	0.56	9.31
aC16	2051.11	166.54	20.92	0.58	8.65
aC18	2457.55	164.83	23.03	0.65	8.07

One can see from the HLB Formula, the HLB values decrease with increase of the molecular weight. So that, if we analyze the HLB values in all tables we see the decreasing of values. And also while analyzing the relationship between the packing parameter and HLB values, we see that they are inversely proportional with each other, if P increases HLB decreases.

Table 3.9 The calculated V, a_0, l_c and P values of ester derivatives of RGD with DFT.

Number of C	**V (Å^3)**	**a_0 (Å^2)**	**l_c (Å)**	**P**	**HLB**
C10	1126.74	165.04	13.76	0.49	11.06
C12	1425.66	165.15	15.98	0.54	10.15
C14	1758.15	164.95	18.19	0.58	9.37
C16	2111.63	166.54	20.35	0.62	8.71
C18	2518.54	164.83	22.57	0.67	8.13

Table 3.10 The calculated V, a_0, l_c and P values of amide derivatives of RGD with DFT.

Number of C	**V (Å^3)**	**a_0 (Å^2)**	**l_c (Å)**	**P**	**HLB**
aC10	1281.59	172.70	12.39	0.59	11.00
aC12	1613.34	175.21	15.29	0.60	10.03
aC14	1972.03	176.35	17.07	0.65	9.31
aC16	2364.96	175.18	19.86	0.68	8.65
aC18	2808.12	176.35	20.14	0.79	8.07

In the truncated cone methods with DFT the P values of amide derivatives are relatively bigger than the ester derivative ones. Because amide derivatives have bigger volume even if the tail height of all amide derivatives are smaller, in general they have bigger P values. It should be noted that l_c and P values are inversely proportional to each other, if l_c increases P decreases.

When HF and DFT results are compared in terms of V and a0 for the same derivatives it is seen that DFT results are relatively bigger than the HF results because HF bonds lenghts are usually too short. For example, if we focuse on aC10 derivative of RGD, while the volume of hydrophobic part is 2457.55 in HF it is 2808.12 in DFT, and while the head group area is 164.83 at HF it is 176.35 DFT. Although V and a_0 values are different at HF, there is no considerable change on the P values because P are in corelation with V,lc and a0. For example, while P is 0.65 at HF it is 0.79 at DFT for

the aC10 derivative. It should be noted that, HF results are acceptable for the P values but this approximation neglects the electron corelation so that HF bond lenghts are too short. If one wants to get more closer results to literature he or she should use DFT because its results are closer the experimental results [2].

Two quantum chemical calculation methods are used in all calculations; HF and DFT. As highlighted in Section 2.2.1.2, DFT results are found to be closer to the experimental results in the literature and therefore they should be examined [2]. The formation of surfactant in aqueous solution in general viewed as a settlement between the tendency for hyrophobic groups to avoid energetically unfavourable contact with water and polar group to maintain contact with aqueous solution [3]. And also, surfactant molecules tend to aggregate as close as possible with each other in the solution. In addition to this information, it is seen that P values calculated with truncated cone method are out of range of Israelachvili model. For all these reasons, the calculations of the volumes by cross-sectional area method should be focused.

In this thesis study, Table 3.9 and Table 3.10 give better understanding about the aggregation behaviour of surfactant in solution. According to model of Israelachvili, the C10, C12 and C14 derivatives which have relatively smaller P values may tend to aggregate to form micelle or they may have intermediate forms between the micelle and vesicle forms because they have P values very close to ½. The other ester derivatives, C16, C18, may tend to form vesicles. If we focus on the amide derivatives, we can see that all derivatives tend to aggregate as vesicle form, maybe except for aC10 derivative because it has a smaller P value which is very close to ½. As mention before, amide bond is stronger than ester bond. If we want achieve more stable vesicle, it may be good to use aC12, aC14, aC16 and aC18 derivatives since they have P values corresponding to the vesicular range. According to the literature, the vesicle is a model system for biological membranes that’s why there is a special interest on the surfactant which has vesicle aggregation [4, 5]. The advantages of using vesciles in drug delivery systems such as reduced number of toxic, maintained therapeutic efficacy of drugs for longer time duration and stability of the vesicular system shouldn’t be ignored [6]. Moreover, the binding of RGD-ligands into vesicles is expected to improve their transfer into cells by binding to specific families of integrins which is most common integrin in brain tumor cells [7]. All makes vesicular system as an ideal drug delivery system.

3.2 THE GRAPH OF V, a_0, l_c AND P VALUES

We can see volume of hyrophobic part and packing parameter for both ester and amide derivatives which optimized at HF/6-31 and DFT/6-31 with two different calculation technics for hyrophobic volume; truncated cone and cross sectional area. And the last graph is HLB values of amide and ester derivatives.

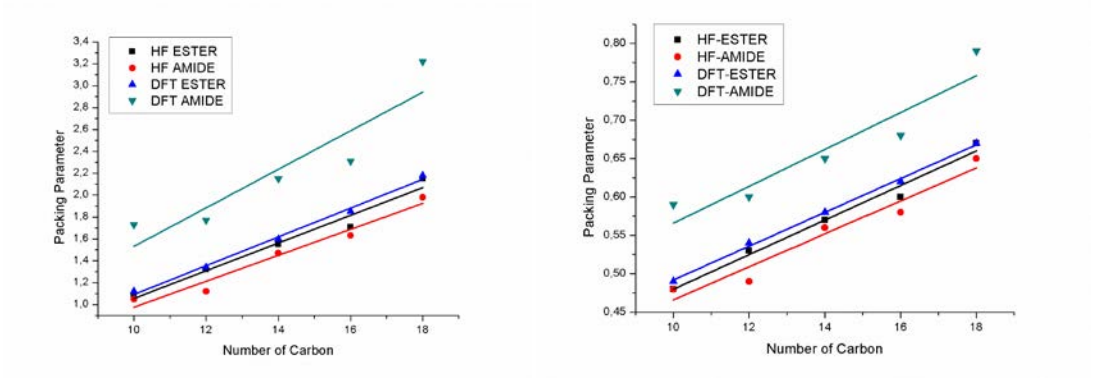

(a) (b)

Figure 3.18 P results (a) truncated cone methods (b) cross-sectional area methods.

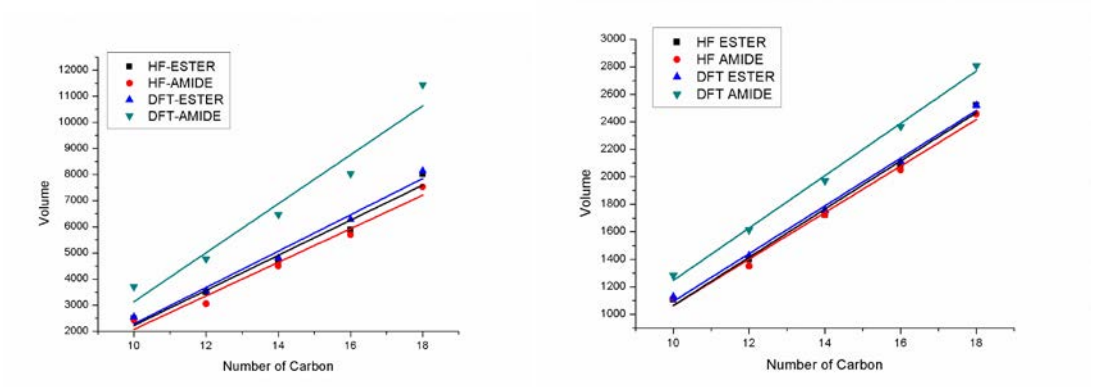

(a) (b)

Figure 3.19 V results (a) truncated cone methods (b) cross-sectional area methods.

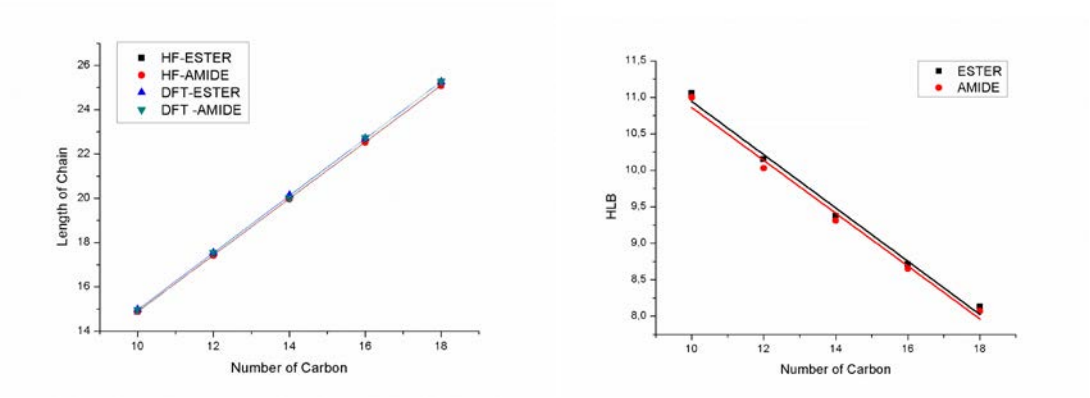

(a) (b)

Figure 3.19 (a) The chain lenght of all molecules and(b) HLB values.

CHAPTER 4

CONCLUSION

In this study, geometry optimizations at the HF/6-311 and B3LYP/6-31 levels of electronic structure theory have been performed for both ester and amide derivatives of RGD. B3LYP method consist of two steps and HF results are used for the second step as initial structure. After optimization part, two different methods are used to calculate the volume of hydrophobic part and P values are calculated. It was investigated that how does packing parameter change depends on the length of the hydrophobic chain. The HF and DFT results are compared in terms of optimized molecular geometries and packing parameters.

Work on RGD tripeptide sequence which selectively affects the αvβ3 integrin protein has a importance. Because αvβ3 integrin is most abundance integrin in brain tumor cells. RGD based drug delivery systems is a promising approach for delivering anticancer drugs or contrast agents for cancer therapy and diagnosis. This is first theoretical study which is about aggregation of RGD tripeptide.

Our continuous experimental studies will show which aggregation type of both ester and amide derivatives of RGD will have exactly. We hoped this study will help of, both experimental and computational studies for double bond compound like RGD.

REFERENCES

[1] Lepzelter, D., Bates, O., and Zaman, M., "Integrin clustering in two and three dimensions", *Langmuir*, Vol. 28(12), pp. 5379-5386, 2011.

[2] Alexander, M., Bendas, G., "*The Role of Adhesion Receptors in Melanoma Metastasis and Therapeutic Intervention Thereof"*, Germany, 2011.

[3] Xiong, J. P., et al., "Crystal structure of the extracellular segment of integrin alphaVbeta3 in complex with an Arg-Gly-Asp ligand", *Science*, Vol. 296(5565), pp. 151-155, 2002.

[4] Demir, A., Synthesis and Biological Investigation of Hydrogenated and Fluorınated Amıno Acıd-Based Molecules that may Bınd Specıfically to the Alpha5/Beta1 Integrın, M.S.Thesis, Fatih University, 2010.

[5] Alberts, B., "*Molecular Biology of the Cell"*, Garland Science, New York, 2008.

[6] Schottelius, M., et al.,Ligands for mapping αvβ3-integrin expression in vivo, *Accounts of Chemical Research*, Vol. 42(7), pp. 969-980, 2009.

[7] Heckmann, D., Design and Synthesis of Selective Ligands for the α5β1 Integrin Receptor and Cyclic Peptides as Affinity Ligands for Factor VIII Purification, Ph.D.Thesis, Technischen Universität München, 2007.

[8] Xiong, X. B., et al., "Enhanced intracellular delivery and improved antitumor efficacy of doxorubicin by sterically stabilized liposomes modified with a synthetic RGD mimetic", *J Control Release*, Vol. 107(2), pp. 262-275, 2005.

[9] Huo, T., et al., "Gd-EDDA/HYNIC-RGD as an MR molecular probe imaging integrin αvβ3 receptor-expressed tumor—MR molecular imaging of angiogenesis", *European Journal of Radiology*, Vol. 73(2), pp. 420-427, 2010.

[10] Marchi-Artzner, V., et al., "Adhesion of Arg-Gly-Asp (RGD) peptide vesicles onto an integrin surface: Visualization of the segregation of RGD ligands into the adhesion plaques by fluorescence", *Langmuir*, Vol. 19(3), pp. 835-841, 2003.

[11] Danhier, F., Breton, A. L., Préat, V., "RGD-based strategies to target alpha(v) beta(3) integrin in cancer therapy and diagnosis", *Molecular Pharmaceutics*, Vol. 9(11), pp. 2961-2973, 2012.

[12] Bergstrand, N., "*Liposomes for Drug Delivery"*, Akademitryck AB, 2003.

[13] Schlegel, H. B., "Geometry optimization", *Wiley Interdisciplinary Reviews: Computational Molecular Science*, Vol. 1(5), pp. 790-809, 2011..

[14] Foresman, B. F., "*Exploring Chemistry withElectronic Structure Methods"*, Pittisburg, 1996.

[15] Karasulu, B., *Reaction Path Analysis of Histone Tail Lysine Residue Demethylation Using Only-QM and Hybrid QM/MM Methods*, M.S. Thesis, Koc University, 2010.

[16] Cortis, C. M., et al., "Quantum mechanical geometry optimization in solution using a finite element continuum electrostatics method", *Journal of Chemical Physics*, Vol. 105(13), pp. 5472-5484, 1996.

[17] Haw, P., "*The HLB System*", USA, 2004

[18] Nagarajan, R., "Amphiphilic surfactants and amphiphilic polymers: Principles of molecular assembly", *American Chemical Society,* Vol: 1070, pp. 1-22, 2011.

[19] Seo, D. S., et al., "Two-dimensional packing patterns of amino acid surfactant and higher alcohols in an aqueous phase and their associated packing parameters", *J Colloid Interface Sci*, Vol. 273(2), pp. 596-603, 2004.

[20] Israelachvili, J., "The Science and Applications of Emulsions -an Overview", *Colloids and Surfaces a-Physicochemical and Engineering Aspects*, Vol. 91, pp. 1-8, 1994.

[21] Consola, S., et al., "Design of original bioactive formulations based on sugar-surfactant/non-steroidal anti-inflammatory catanionic self-assemblies: a new way of dermal drug delivery", *Chemistry,* Vol. 13(11), pp. 3039-3047, 2007.

[22] Israelachvili, J. N., Mitchell, D. J., Ninham, B. W., "Theory of self-assembly of hydrocarbon amphiphiles into micelles and bilayers", *Journal of the Chemical Society-Faraday Transactions Ii*, Vol. 72, pp. 1525-1568, 1976.

[23] Hehre, W. J., *A Guide to Molecular Mechanics and Quantum Chemical Calculations,* Wavefunction, United States of America, 2003.

[24] Chang, T., Gao, H., "Size-dependent elastic properties of a single-walled carbon nanotube via a molecular mechanics model", *Journal of the Mechanics and Physics of Solids*, Vol. 51(6), pp. 1059-1074, 2003.

[25] KARACA, S.,*The Study Of Ground State And Excıted State Propertıes Of Cyanıne Dyes By Usıng Computatıonal Chemıcal Methods*,M.S. Thesis, The Graduate School of Engineering and Science of İzmir Institute of Technology, 2008.

[26] Atkins, P., Friedman, R., "*Molecular Quantum Mechanıcs"*, Oxford University Press, New York, 2005.

[27] Sherrill, C. D., "*Introduction to Molecular Mechanics"*, Georgia Institute of Technology

[28] Shattuck, T. W., "*Molecular Mechanics Tutorial*", Waterville, Maine, 2008.

[29] Szabo, A., Ostlund, N. S., "*Modern Quantum Chemistry: İntroduction To Advanced Electronic Structure Theory*": McGraw-Hill Publishing Company,New York, 1989.

[30] Burke, K., et al., "*The ABC of DFT "*, California,2007.

[31] http://newton.ex.ac.uk/research/qsystems/people/coomer/dft_intro.html.

[32] Yang, R. G., Yang, W., "*Density-Functional Theory of Atoms and Molecules*",Oxford University Press, New York, 1989.

[33] Blaber, M., "*Biochemistry I*", Florida State University, 2001

[34] Akar, I., *Investigatıon of 5-Chloro-8-Hidroksikinolin and Zn and Mn Complexes by Theoretical and Experimental Vibrational Spectroscopy*, M.S. Thesis, Kilis University, 2011.

[35] Schramm, L. L., *"Surfactants: Fundamentals and Applications in the Petroleum Industry*" Cambridge University Press, 2000.

[36] Sun, T., et al., "Stable vesicles assembled by “supramolecular amphiphiles” with double hydrophobic chains", *Colloids and Surfaces A: Physicochemical and Engineering Aspects*, Vol. 414(0), pp. 41-49, 2012.

[37] Lehn, J. M., "Toward complex matter: supramolecular chemistry and self-organization", *Proc Natl Acad Sci U S A*, Vol. 99(8), pp. 4763-4768, 2002.

[38] Saurabh, B., at al., "A comparative review on vesicular drug delivery system and stability issues",*Internatıonal Journal Of Research In Pharmacy And Chemıstry*, ISSN: 2231-2781, 2012.

[39] Marchi-Artzner, V., et al., "Adhesion of Arg-Gly-Asp (RGD) Peptide Vesicles onto an Integrin Surface: Visualization of the Segregation of RGD Ligands into the Adhesion Plaques by Fluorescence", *Langmuir*, Vol. 19(3), pp. 835-841. 2002.